

Photon-to-Digital Converters – A 3D Integrated Digital Single-Photon Detector for Large Scale Photodetection Systems and more...

Serge A. Charlebois¹, Fabrice Retiere², Jean-François Pratte¹
for the **GRAMS3D** research group

¹ Université de Sherbrooke, Canada

² TRIUMF, Vancouver, Canada

TRIUMF Science Week, July 2025

Université de Sherbrooke

Jean-François Pratte

Serge Charlebois

Artur Turala

Frédéric Nolet

Frédéric Vachon

Gabriel Lessard

Guillaume Théberge-Dupuis

Jeanne Morehead

Jérémy Chenard

Jérôme Deshaies

Keven Deslandes

Nicolas Roy

Philippe Arsenault

Philippe Martel-Dion

Raffaele Aaron Giampaolo

Robin Scarpellini

Samuel Parent

Sean Prentice

Simon Carrier

Tommy Rossignol

Olivier Lepage

Yves-Alexandre Beebe

Collaborators

Fabrice Retiere (TRIUMF)

Thomas Jennewein

QEYSSAT

Lorenzo Fabris (ORNL)

QKD Micro-net

Stéphane Martel (TDSI)

Jean-Pierre Veran (NRC)

Simon Viel (Carleton)

Steve Maclean (IPlabs)

Pierre Lévesque (IPlabs)

nEXO Collaboration

nEXO Canada

ARGO Collaboration



- Scintillating crystal-based systems

- Positron Emission Tomography
 - Computed Tomography
 - Neutron Imaging
- Precise single-photon timing resolution
- Visible spectrum

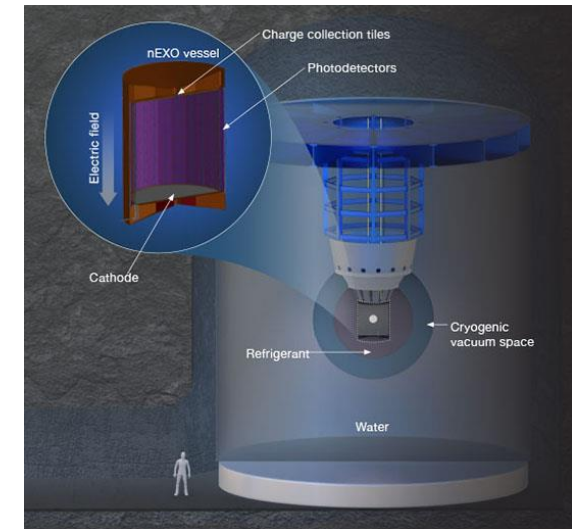


Mid-sized Animal LabPET II

- Noble liquid experiments (Argon and Xenon)

- Dark matter search
 - Neutrino physics
- Large area detector ($\sim \text{m}^2$)
→ Low power
- VUV sensitivity

5 to 100s m^2 of detector area!

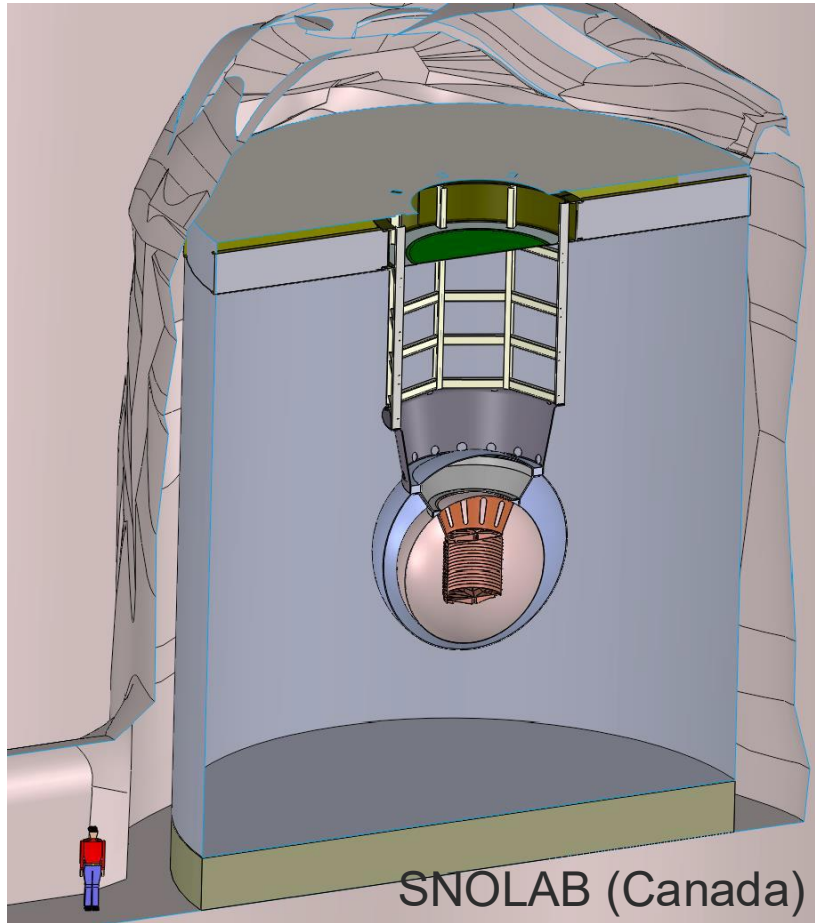


The nEXO time projection chamber (top left inset) allows measurement of energy and location of double beta decays.

<https://nexo.llnl.gov>

nEXO – neutrino search

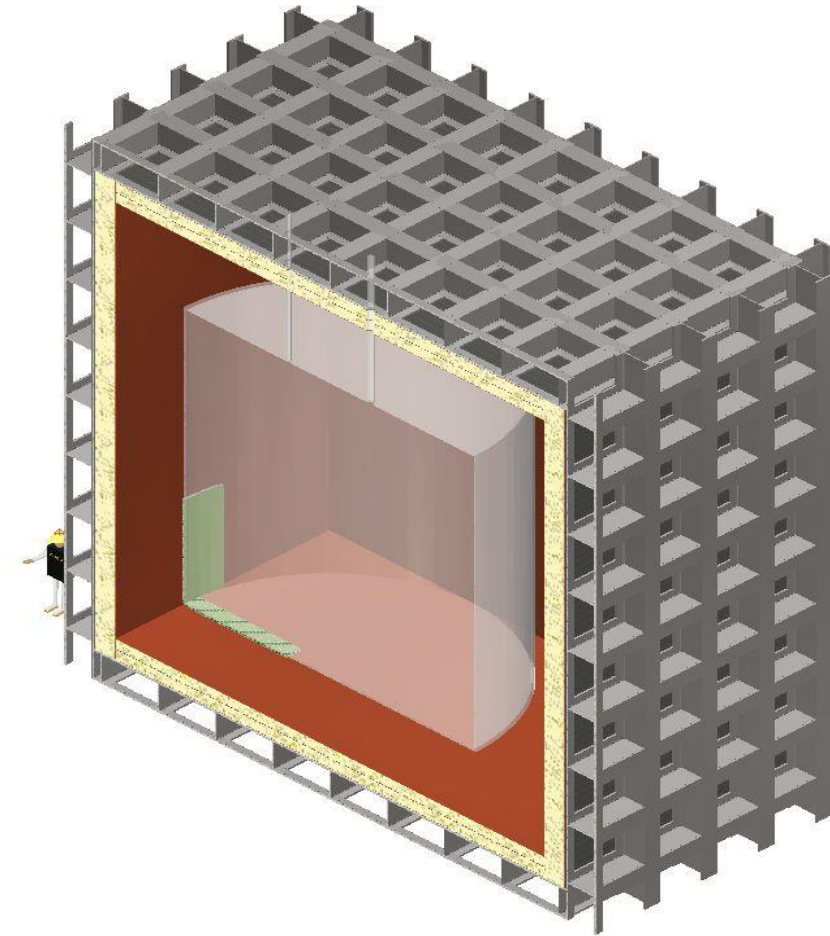
^{136}Xe $0\nu\beta\beta$ decay – xenon as scintillator



5 tonnes of LXe – 4.5 m² of photon detectors

ARGO – dark matter search

LAr as interaction media and scintillator

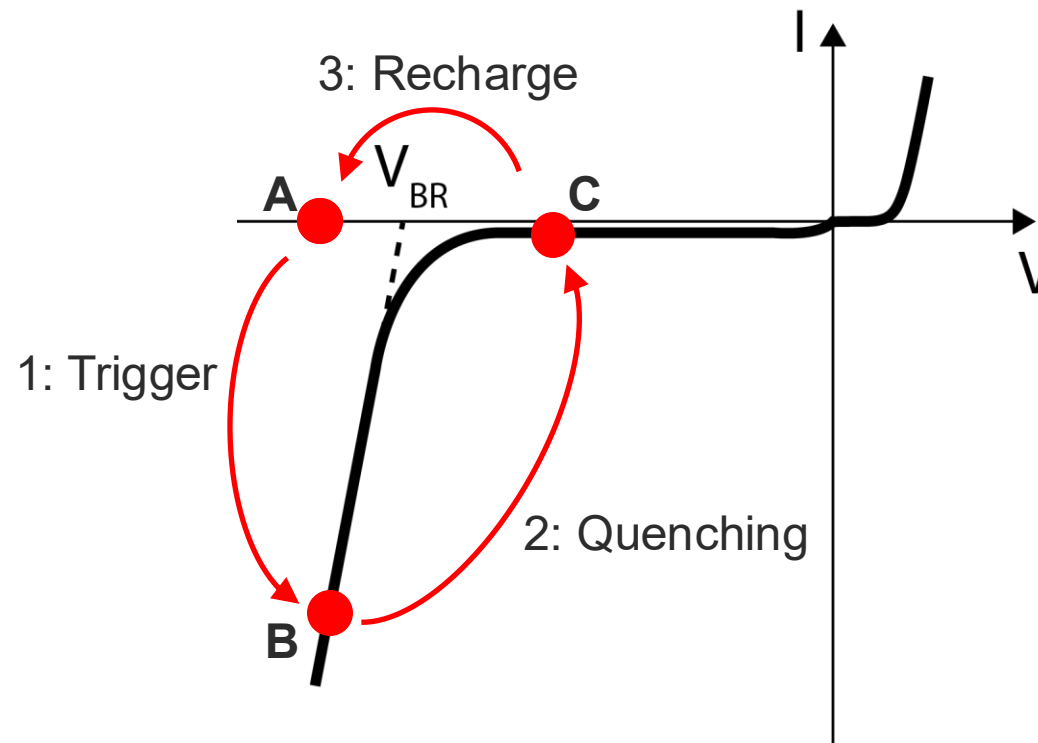
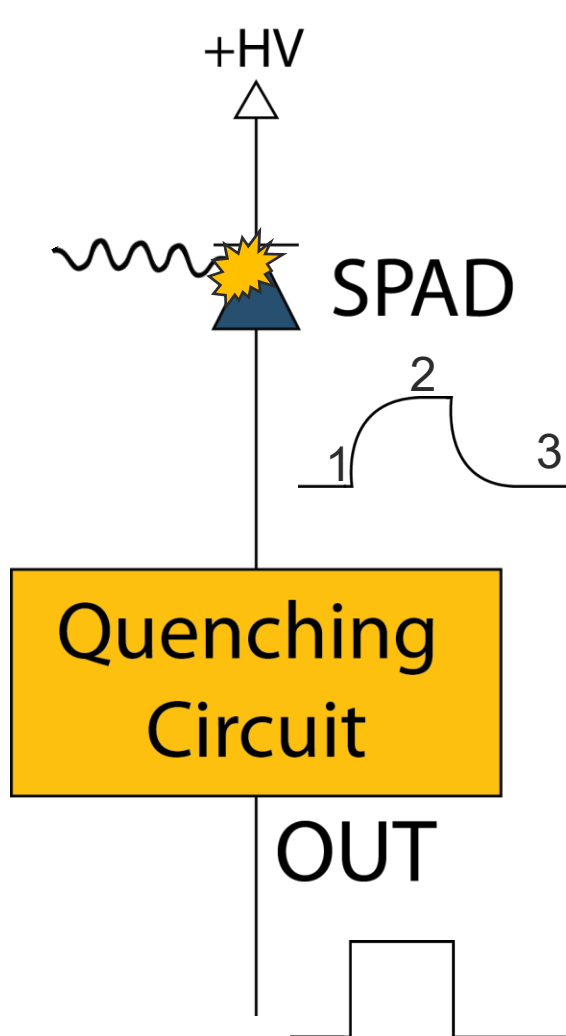


300 tonnes of LAr – 250 m² of photon detectors



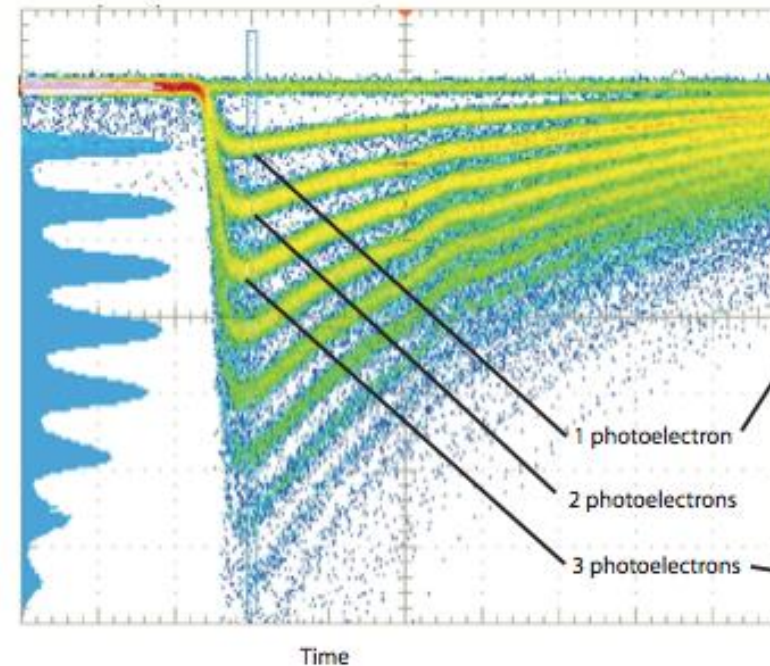
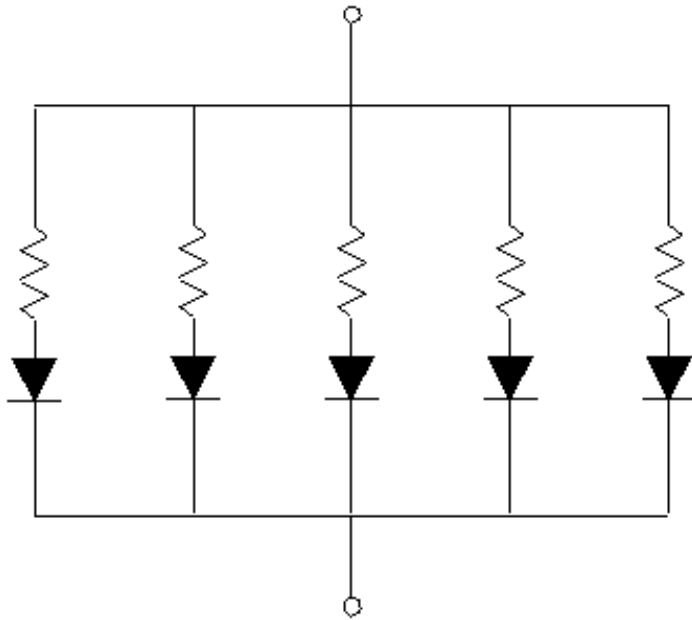
The Photon-to-Digital Converter Concept

How to turn a single photon into a digital pulse

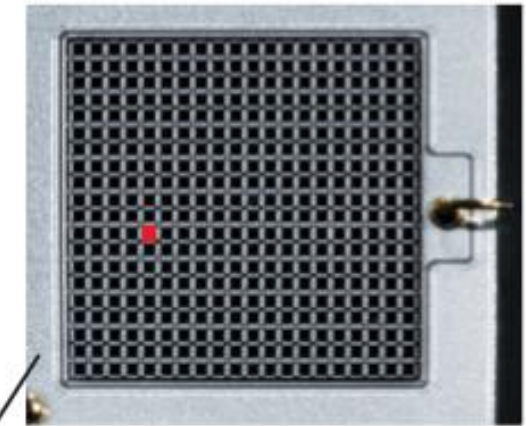


1. Time precision
2. Sensitivity – gain $>10^5$ – single photon
3. Low cost

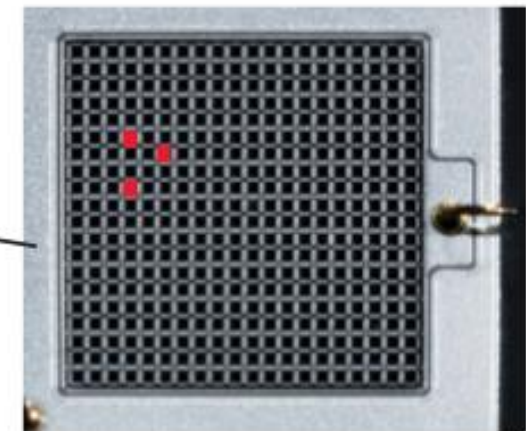
- Array of SPADs in parallel quenched passively



Persistence trace on an oscilloscope



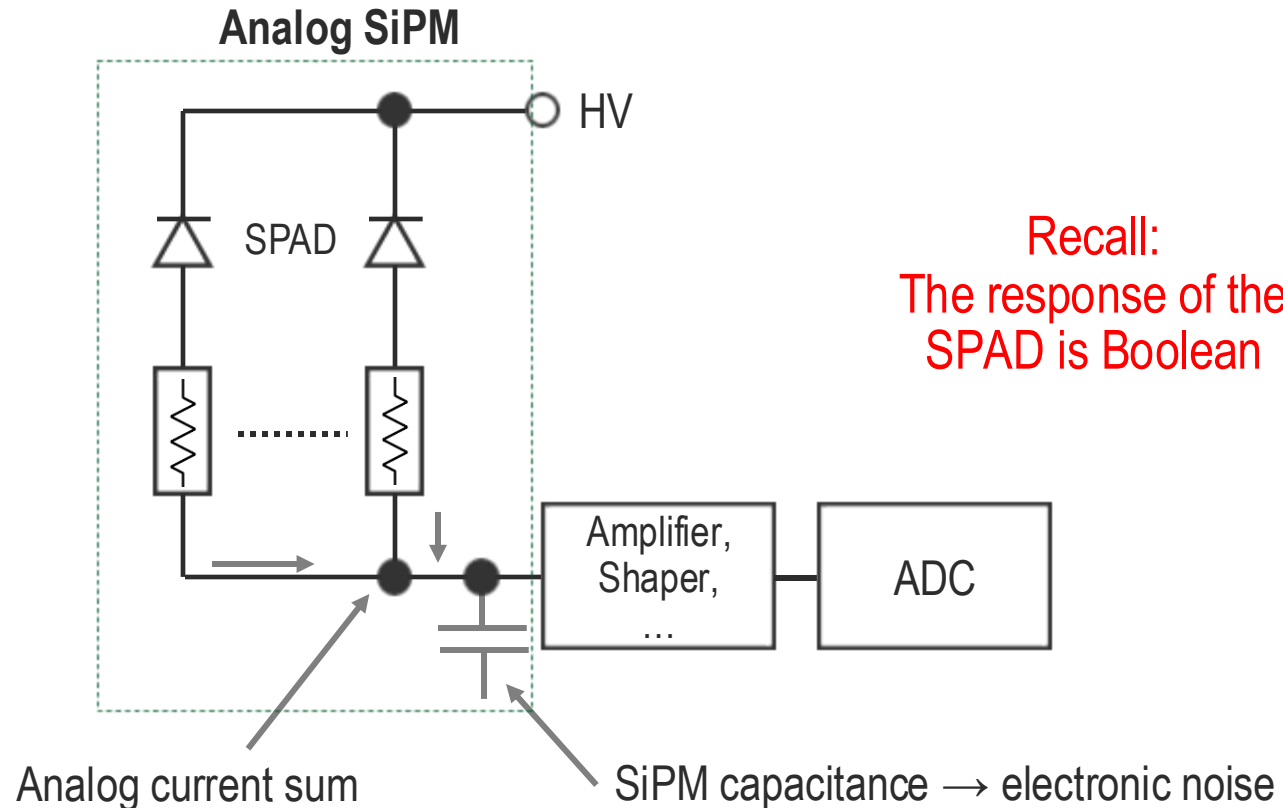
1 Geiger-mode APD activated



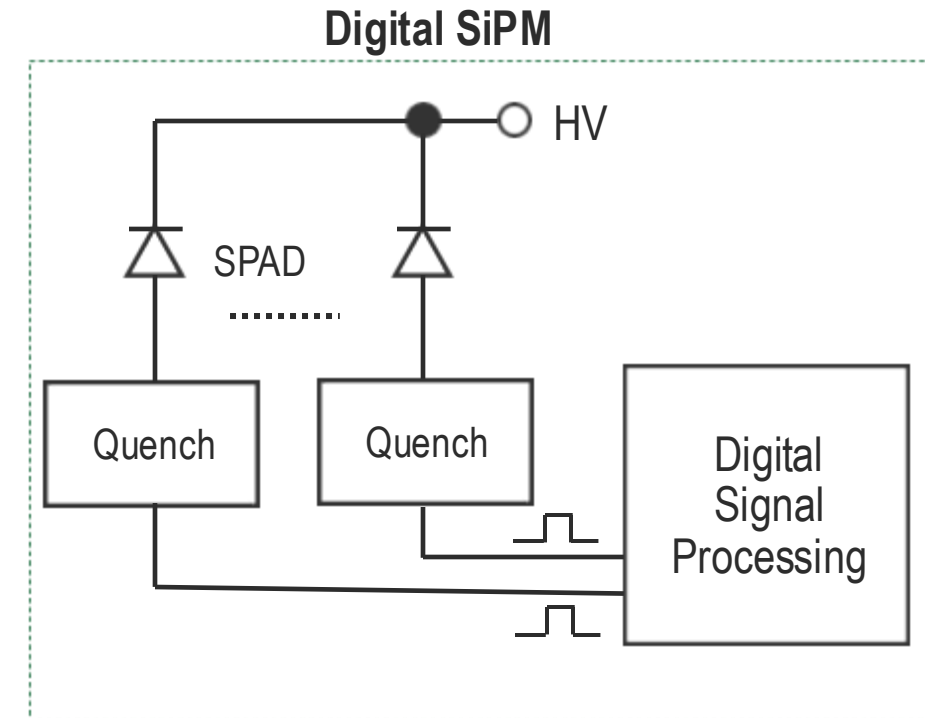
3 Geiger-mode APDs activated

Source: Hamamatsu

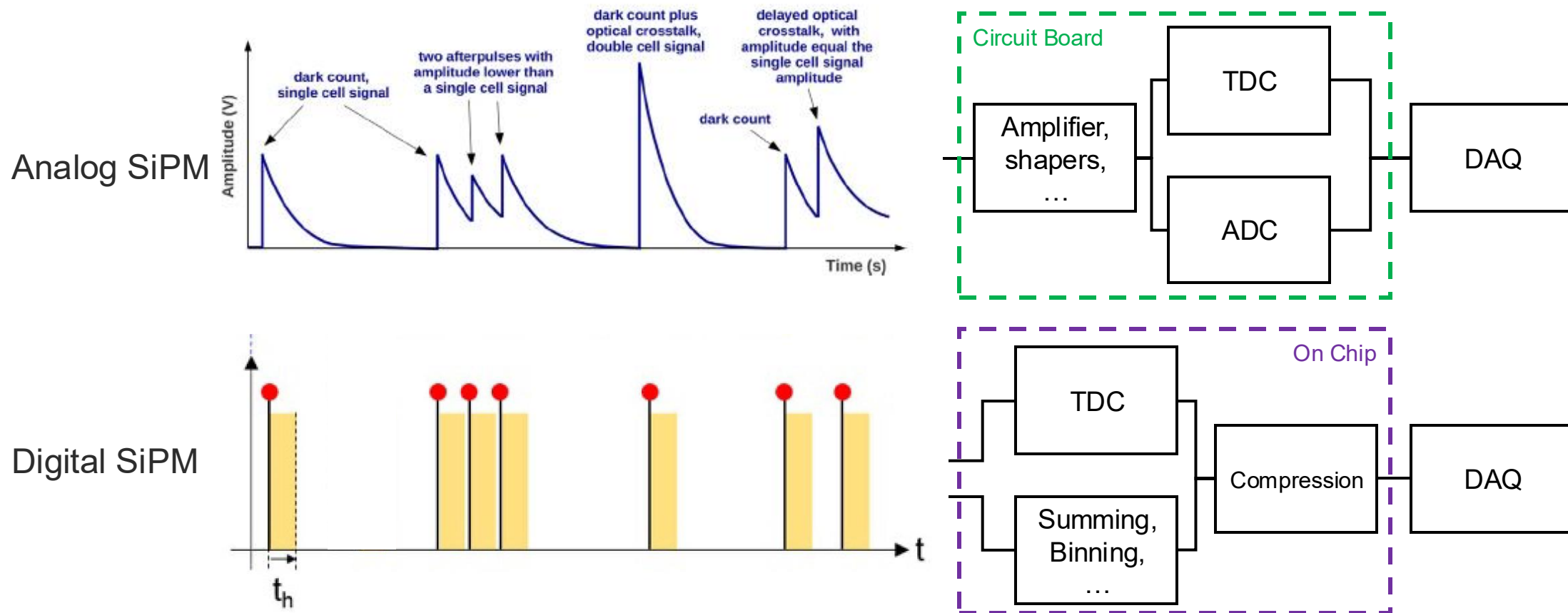
SiPM – Silicon Photo Multiplier: an array of SPADs



The amplifier transforms charge into voltage and then BACK to digital.



Individual SPAD readout, no D/A+A/D conversion. Everything stays digital.



Are the individual photon pulse shapes really needed?
(with all their complications to analyse)

Panel discussion on Wednesday 11h30

Science Technology:

When will digital SiPM move beyond the R&D phase for subatomic physics and other applications?



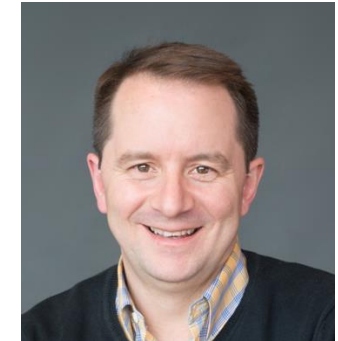
Nicolas D'Ascenzo
Huazhong University of
Science and Technology
China



Peter Fischer
Heidelberg University
Germany



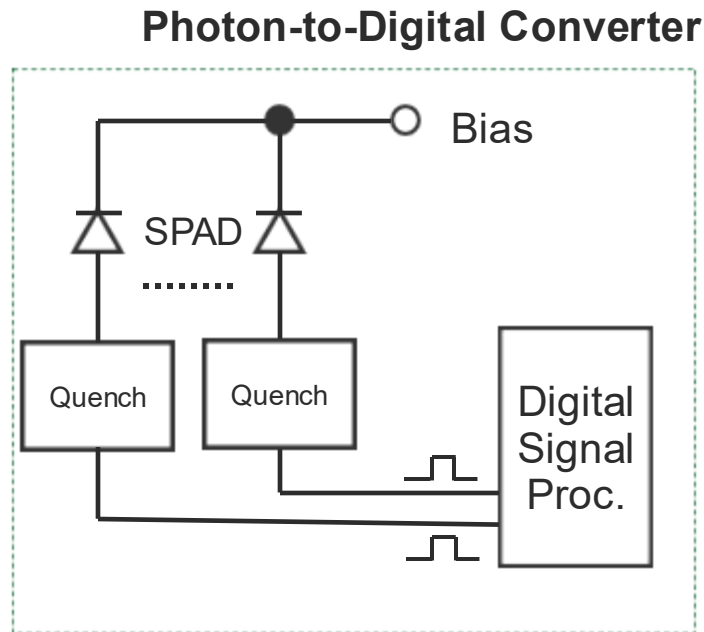
Fabrice Retiere
TRIUMF/Simon Fraser U.
Canada



Serge Charlebois
Université de Sherbrooke
Canada

Questions and opinions and welcome!!!

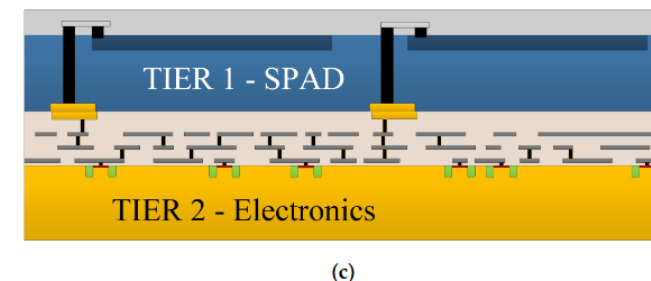
- Digitally readout array of Single Photon Avalanche Diode (SPAD)



- Direct digital conversion:
 - Single photon resolution on the whole dynamic range
 - Can lower power significantly consumption
- Disabling noisy SPADs: reducing noise
- Programmable hold-off delay: mitigation of afterpulsing
- Embedded signal processing: sum, dark count filters, time-to-digital conversion, etc.

Pratte JF et al. "3D Photon-to-Digital Converter for Radiation Instrumentation: Motivation and Future Works" (2021) Sensors;21(2):598. doi: 10.3390/s21020598

- SPAD array and CMOS readout vertically stacked (3D) to form a single detector chip



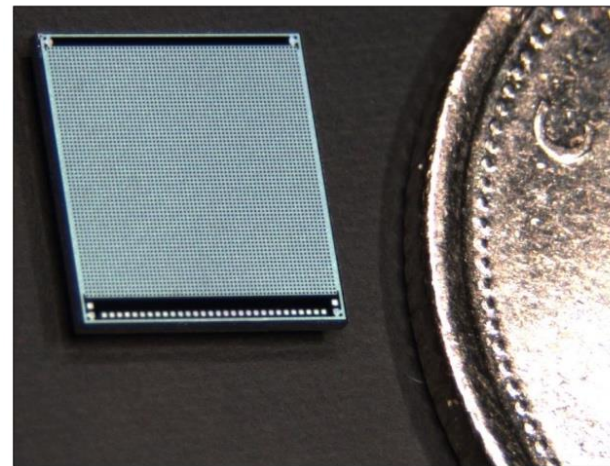
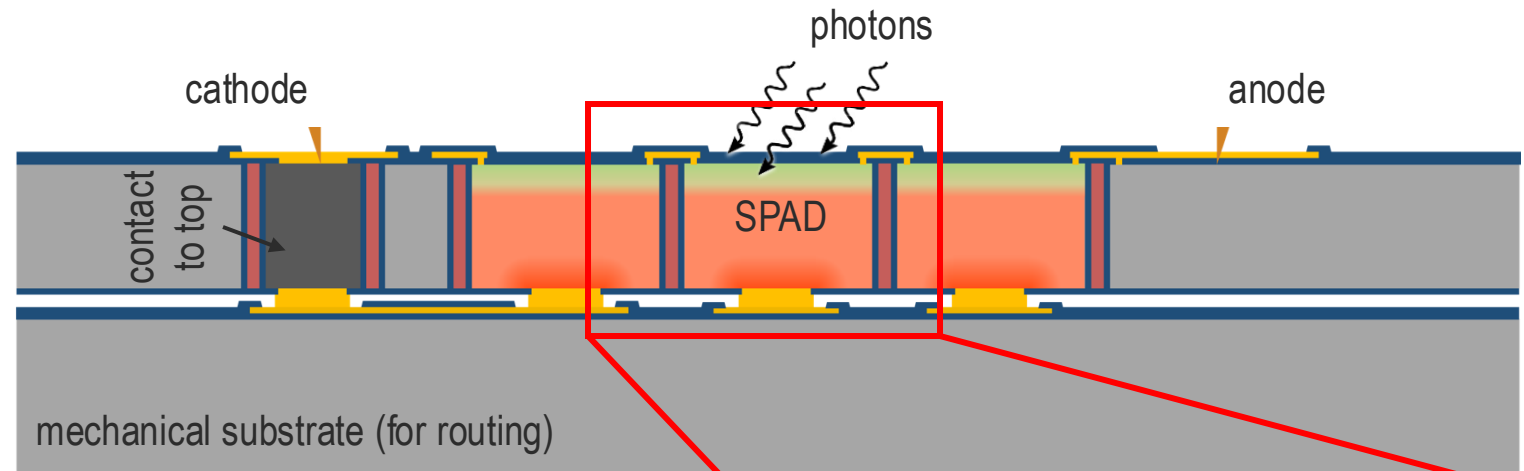


Development of the SPAD array layer and low power PDC

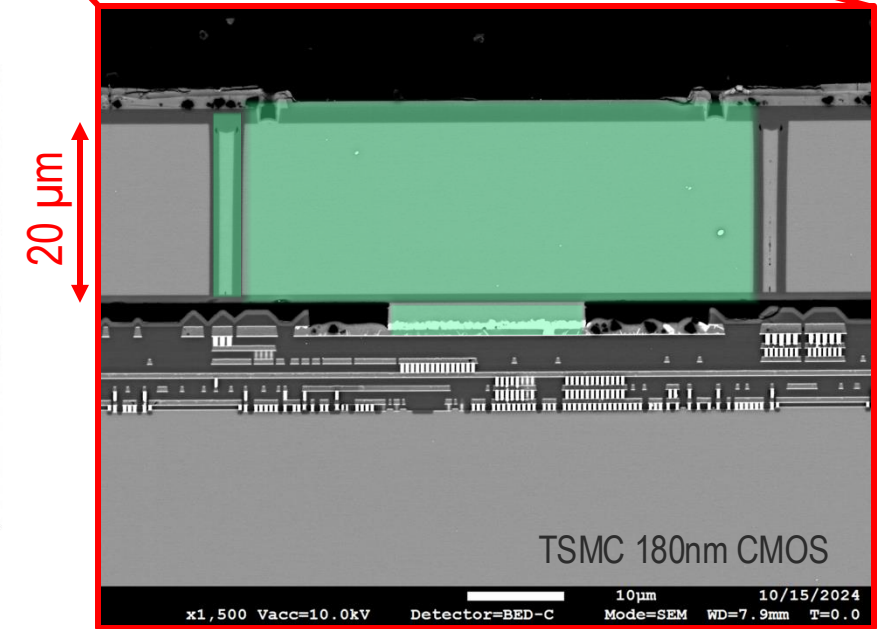
1st fabrication run completed
(Octobre 2024)

Thin SPAD layer + CMOS readout

- p⁺n SPAD [1]
- 64 × 64 SPAD Array
- 78 μm pitch
- Al-Ge eutectic bonding
- 5.85 × 5.25 mm² die

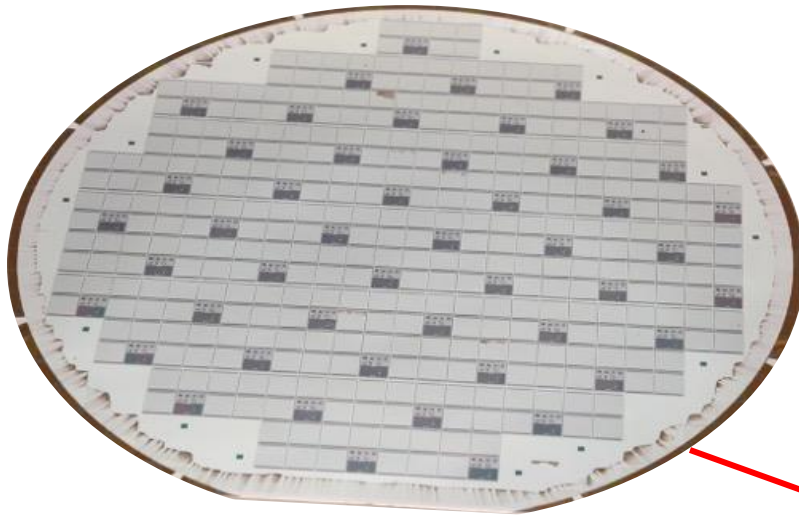


3D SPAD array
(canadian 10¢ for reference)



SEM cross section image

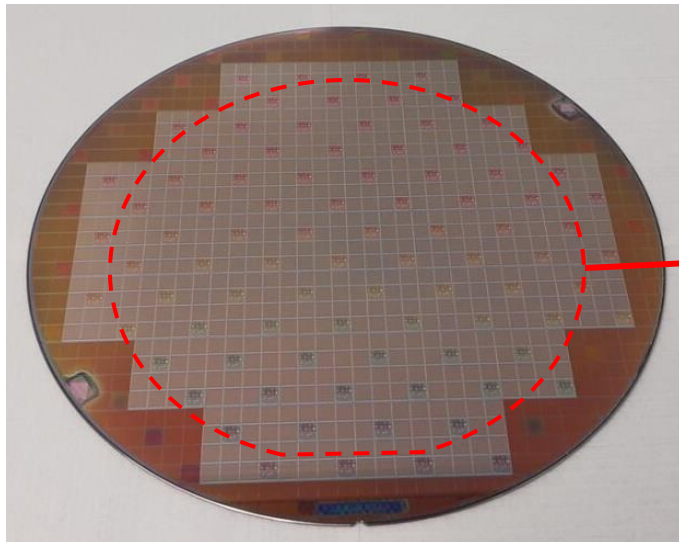
1. Parent, Samuel, et al. "Single photon avalanche diodes and vertical integration process for a 3D digital SiPM using industrial semiconductor technologies." 2018 IEEE Nuclear Science Symposium and Medical Imaging Conference Proceedings (NSS/MIC). IEEE, 2018.



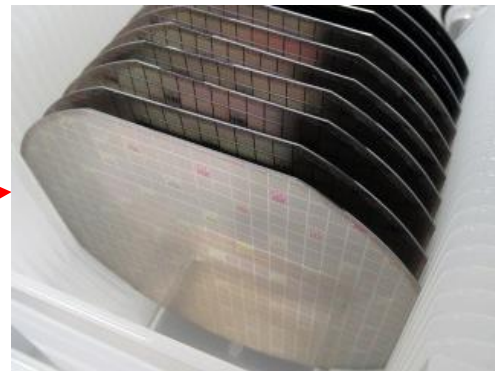
150 mm SPAD wafer

Wafer level bonding

- Al-Ge eutectic: CMOS aluminum pad to SPAD Ge
- Resizing 200 mm to 150 mm (while matching patterns)



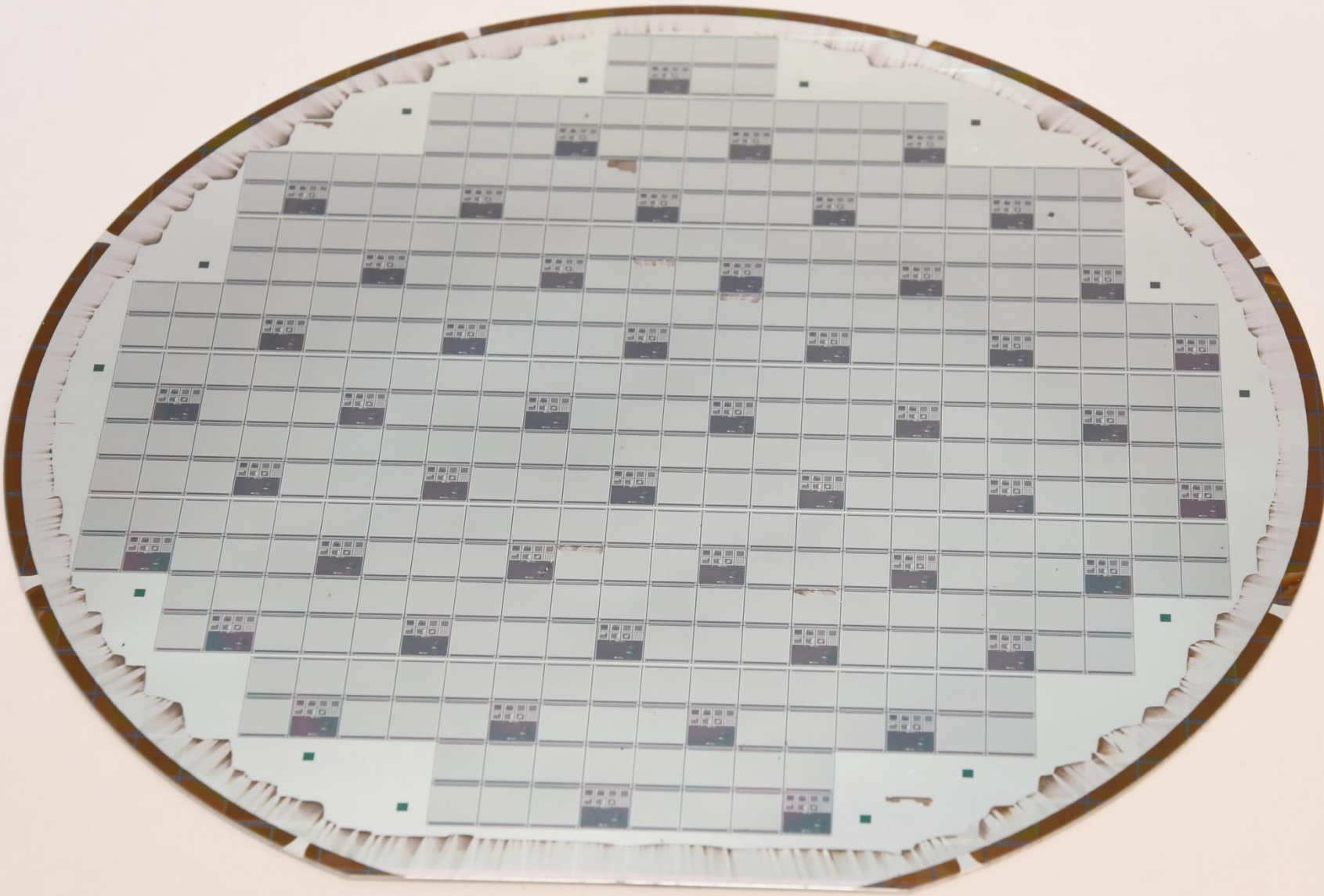
200 mm TSMC 180 nm CMOS wafer



Resized to 150 mm



CMOS readout wafer

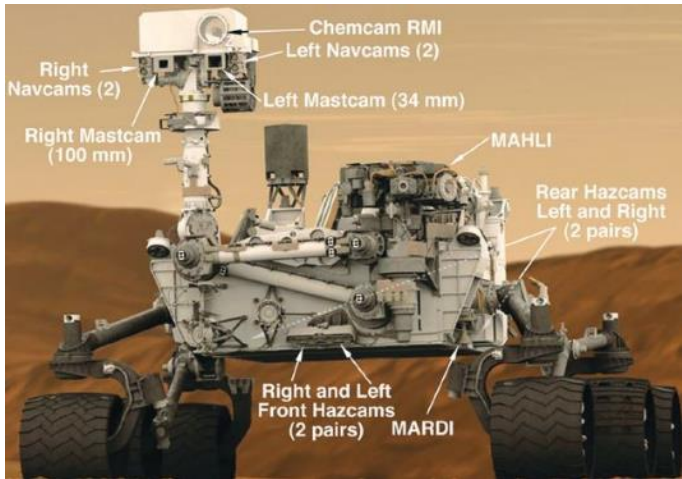


High-end CCD process line

- > excellent for SPAD R&D
- 150 mm process line
- low contaminant / gold free clean rooms

World top 5 MEMS Foundry

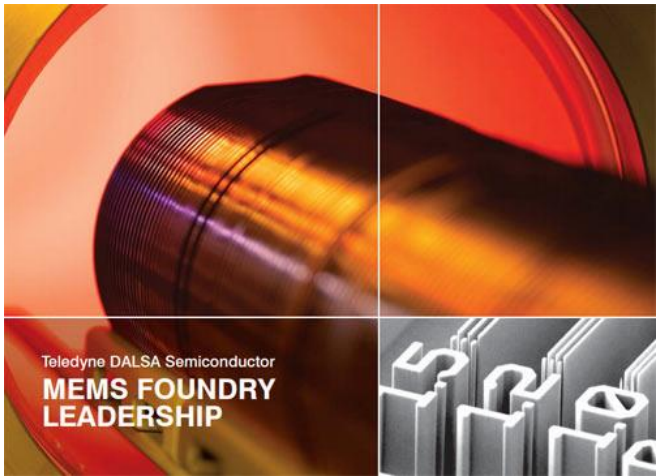
- > excellent for wafer level integration
- 150 mm and 200 mm process line
- Wafer thinning, deep etching, bonding, ...



The Eyes of the Mars Curiosity Rover. Tech Briefs (2012)



Life on Mars: Rover landing gives boost to Canadian tech sector. The Globe and Mail (2012)



Courtesy of Teledyne DALSA

**MEMS Foundry Rankings
(2017 sales in US\$M)**

STMicroelectronics	174
Teledyne DALSA	60
Silex Microsystems	50
TSMC	47
X-Fab	42

*Status of the MEMS Industry 2018
Market and technology Report
Yole Development (2018)*



TELEDYNE DALSA
Everywhere you look™

Teledyne DALSA Semiconductor (est. 1980)
~ 500 employees located at Bromont near Montreal, Canada



**PDC designed for
low power use
in noble liquid experiments**

Flag output

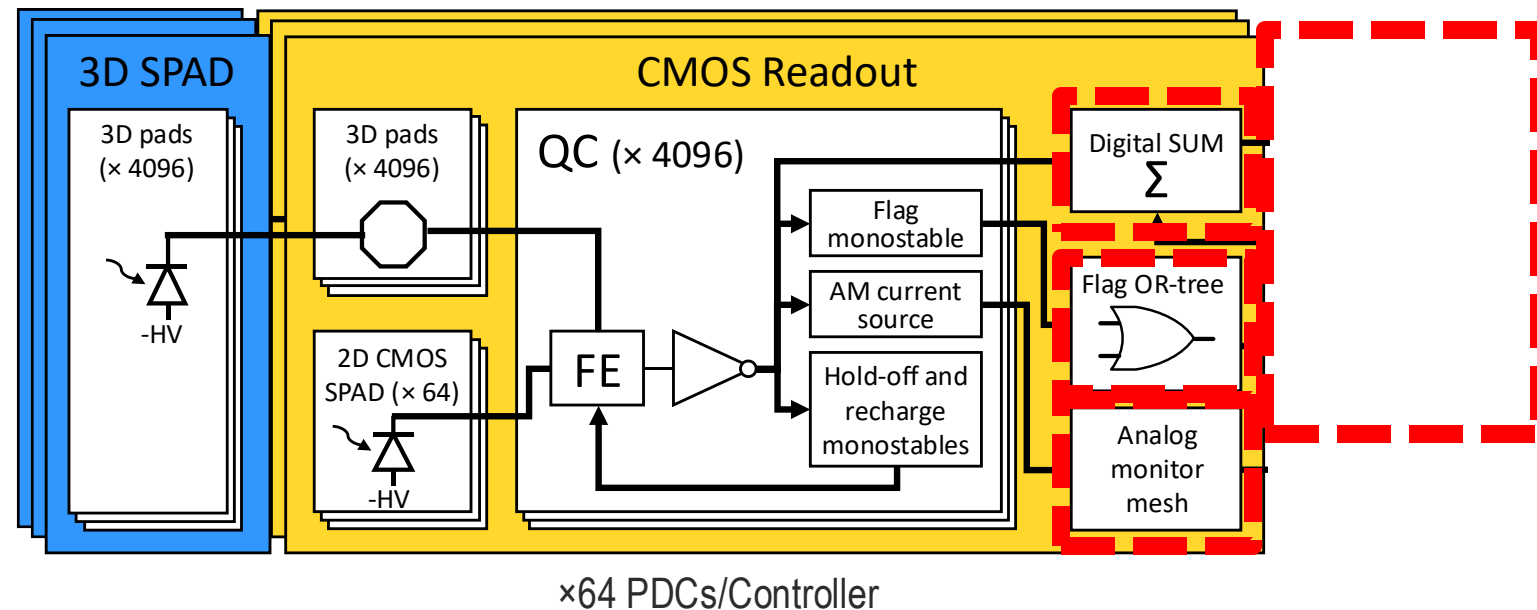
- Pulsed output (adjustable from few ns to tens of ns).
- From an OR-tree.
- Timing jitter better than 100 ps RMS.

Digital Sum

- Digital count of triggered SPADs inside a bin (dynamic range of 4096 photons).
- Adjustable bin width from 10 ns up to μ s.
- Internal FIFO of 128 bins.

Analog Monitor

- Current proportional to triggered SPADs.



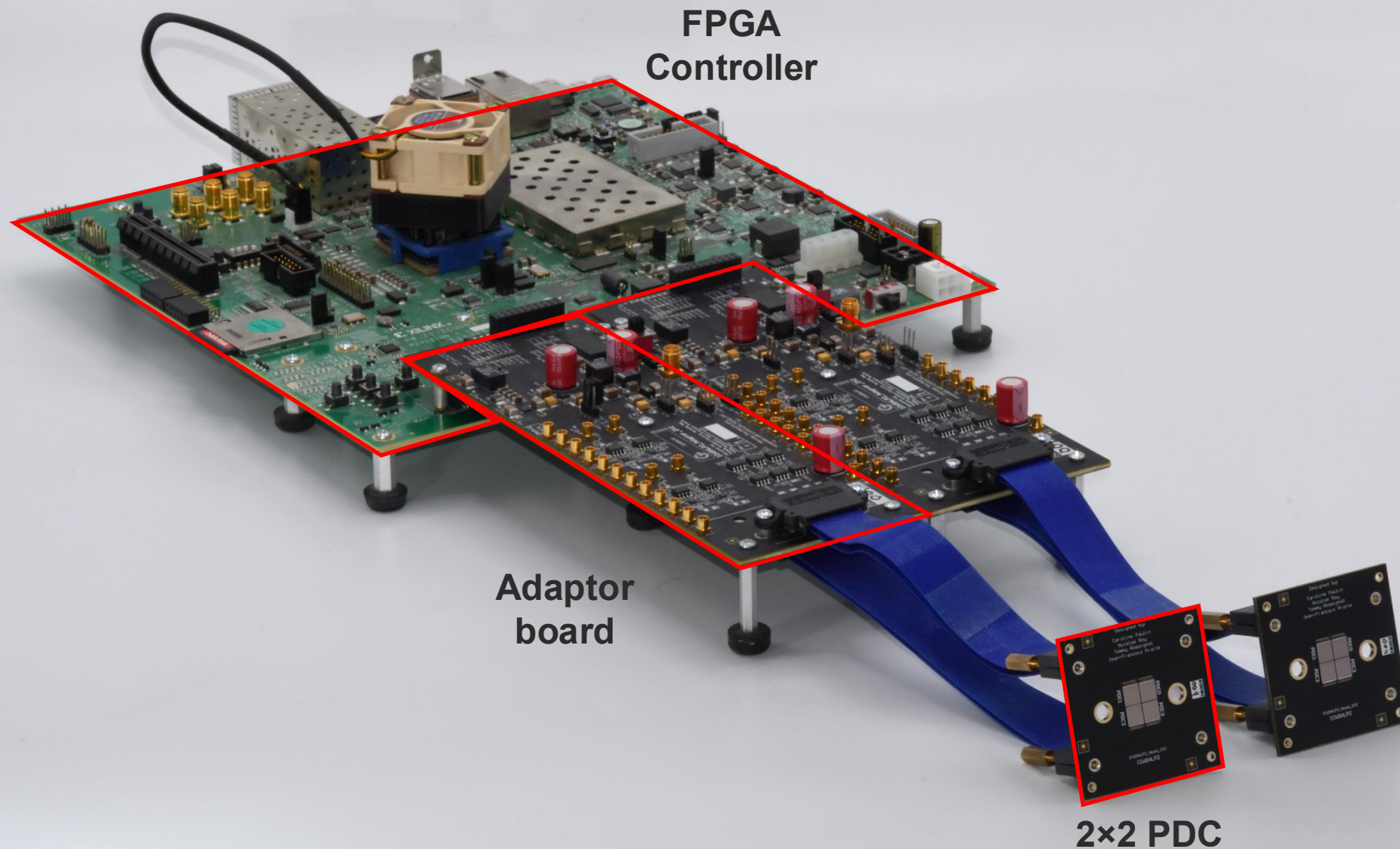
Controller (1 for 64 PDCs)

- Start PDC acquisition, based on the number of flag received to discriminate dark count.
- Bank of TDCs for timing measurements on flags.
- Receives data from PDCs and includes post-processing.
- Communicate with an external computer.



PDC technology dissemination:

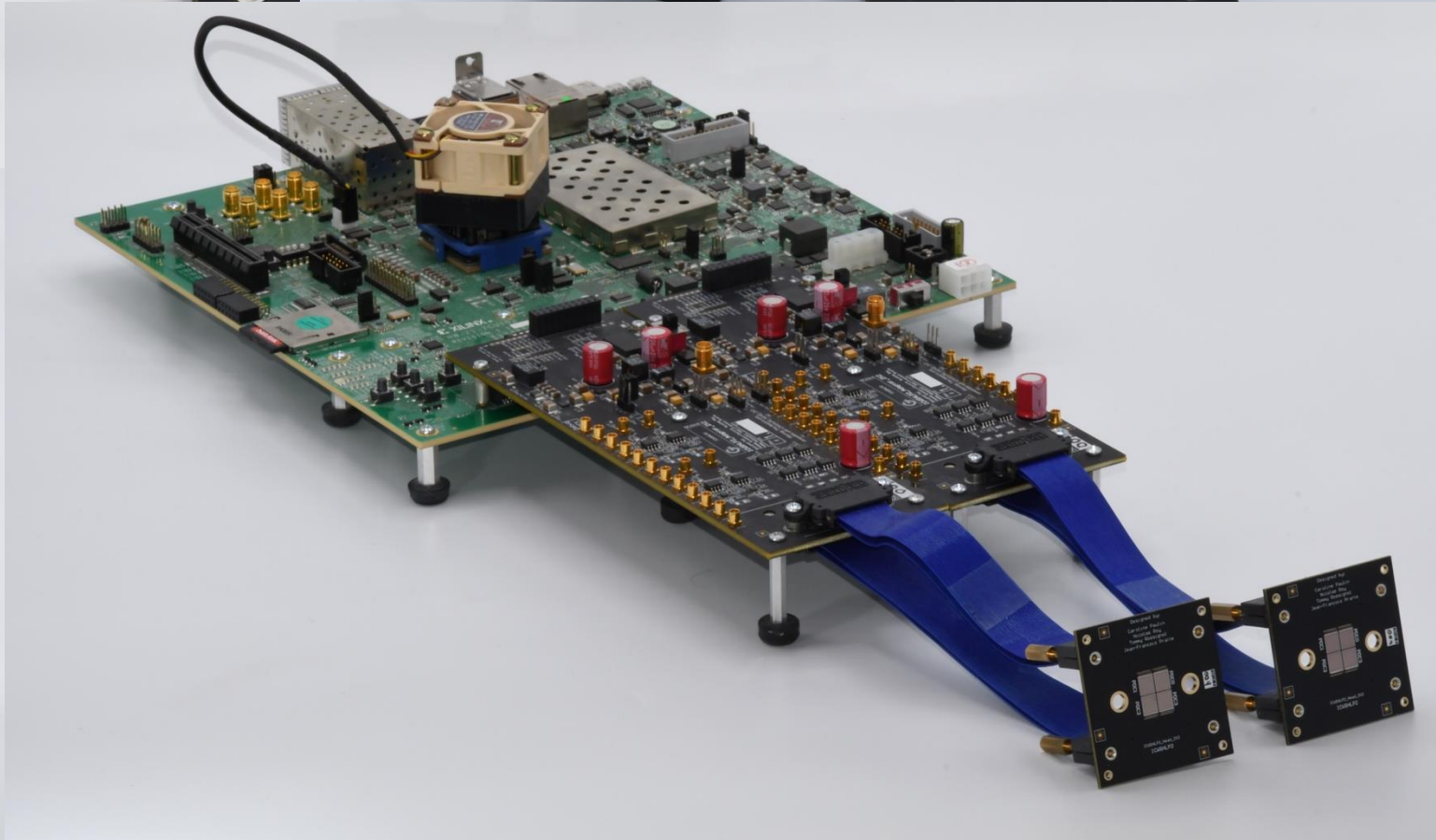
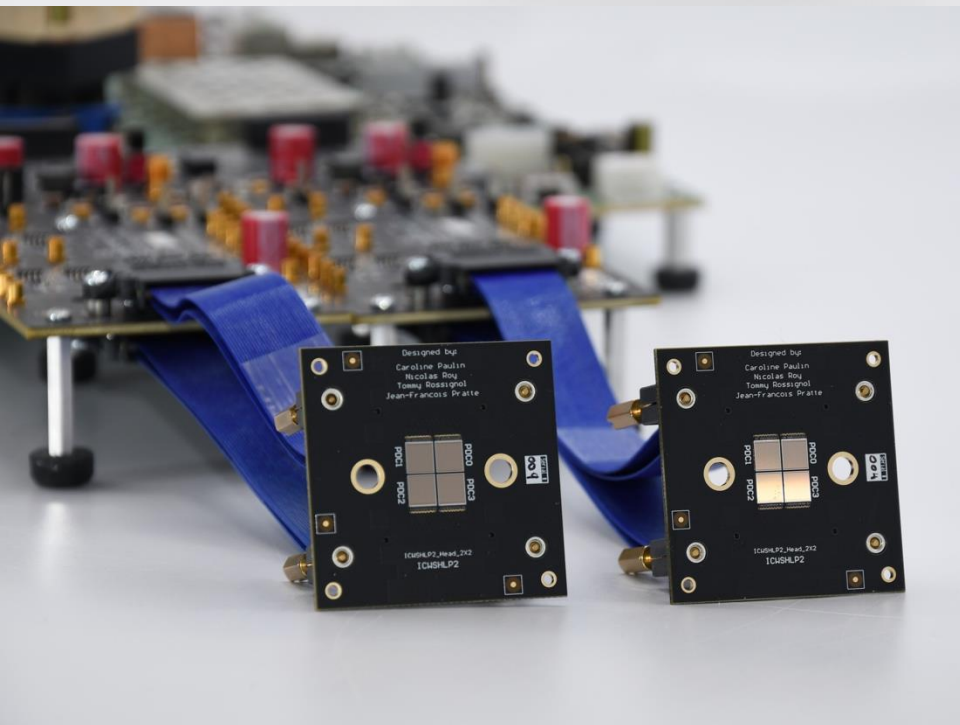
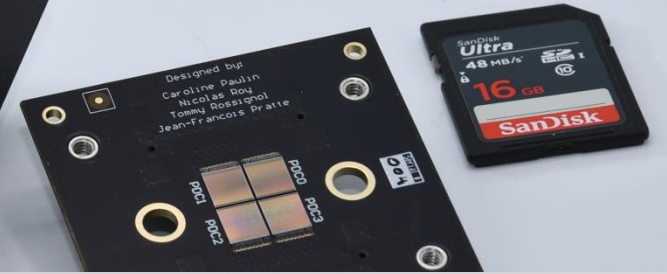
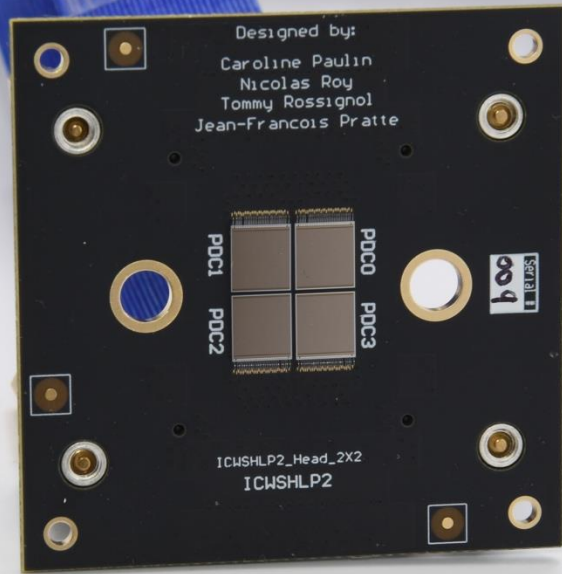
**Sharing a test platform
to allow collaborators
to explore the technology**



Low power Photon-to-Digital Converter

For details, see T. Rossignol et al., J. Inst., vol. 19, no. 09, p. P09017, Sep. 2024

<https://doi.org/10.1088/1748-0221/19/09/P09017>



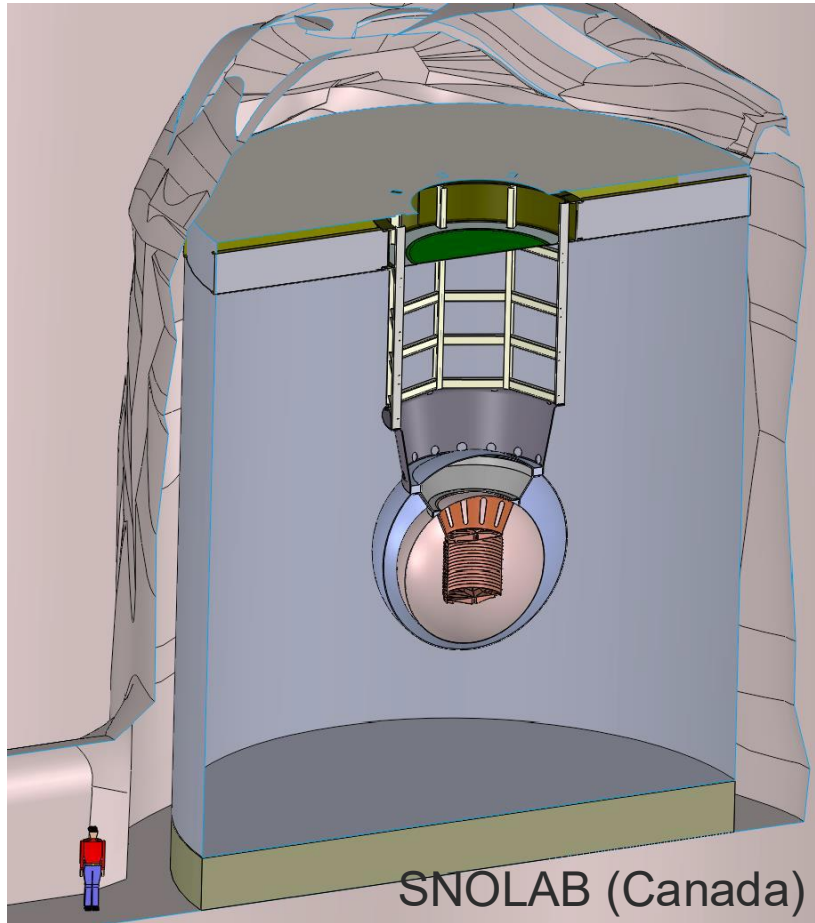


Our global research program:

Photon Detection Modules

nEXO – neutrino search

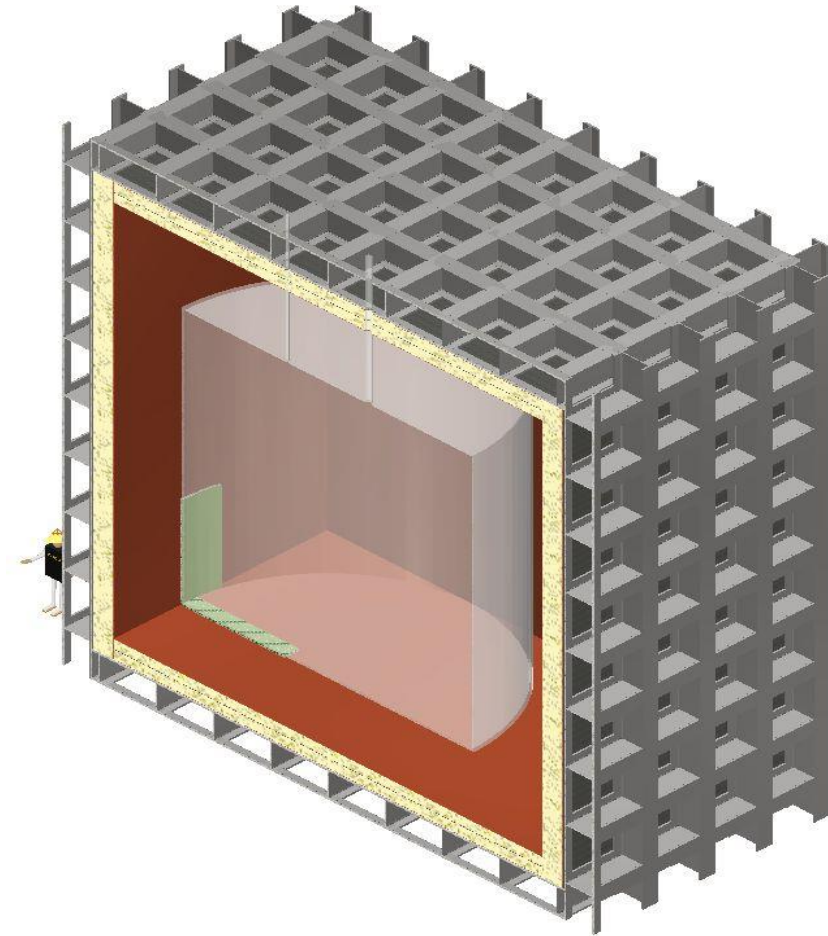
^{136}Xe $0\nu\beta\beta$ decay – xenon as scintillator



5 tonnes of LXe – 4.5 m² of photon detectors

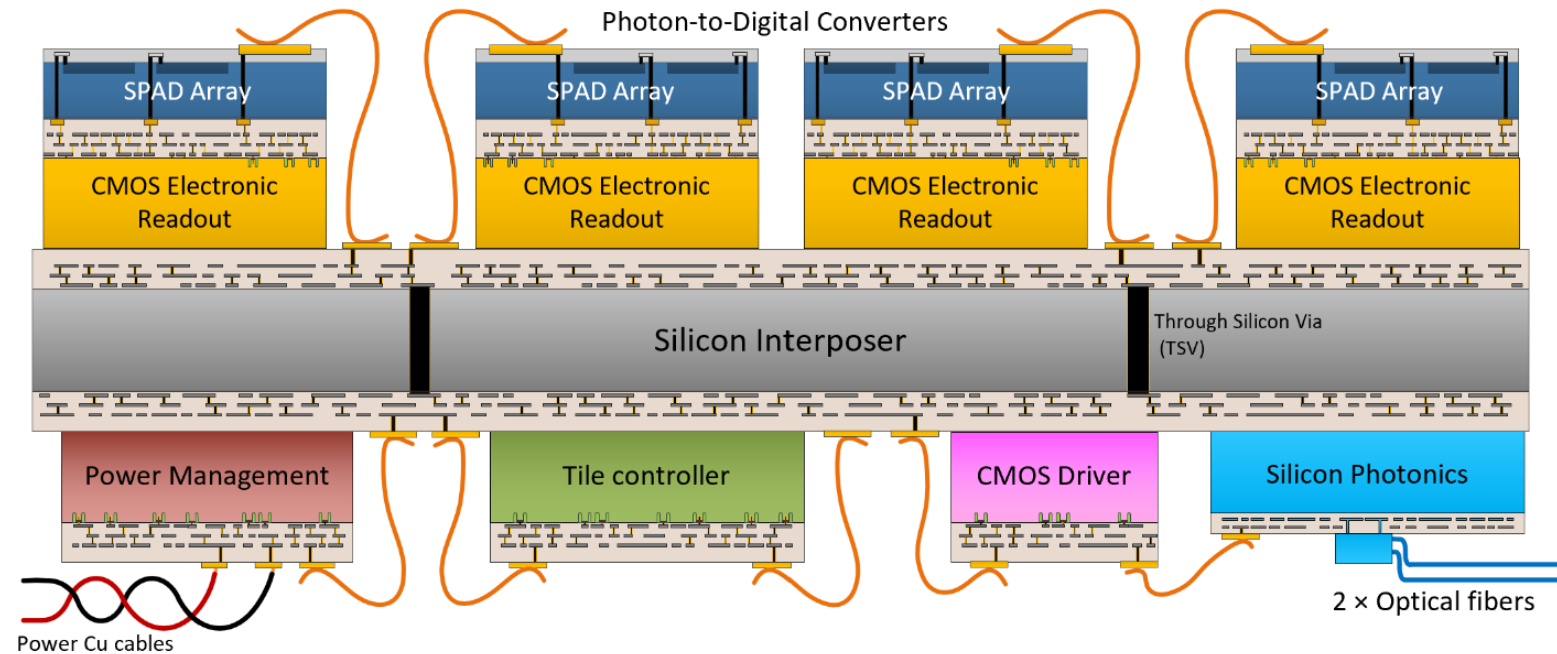
ARGO – dark matter search

LAr as interaction media and scintillator



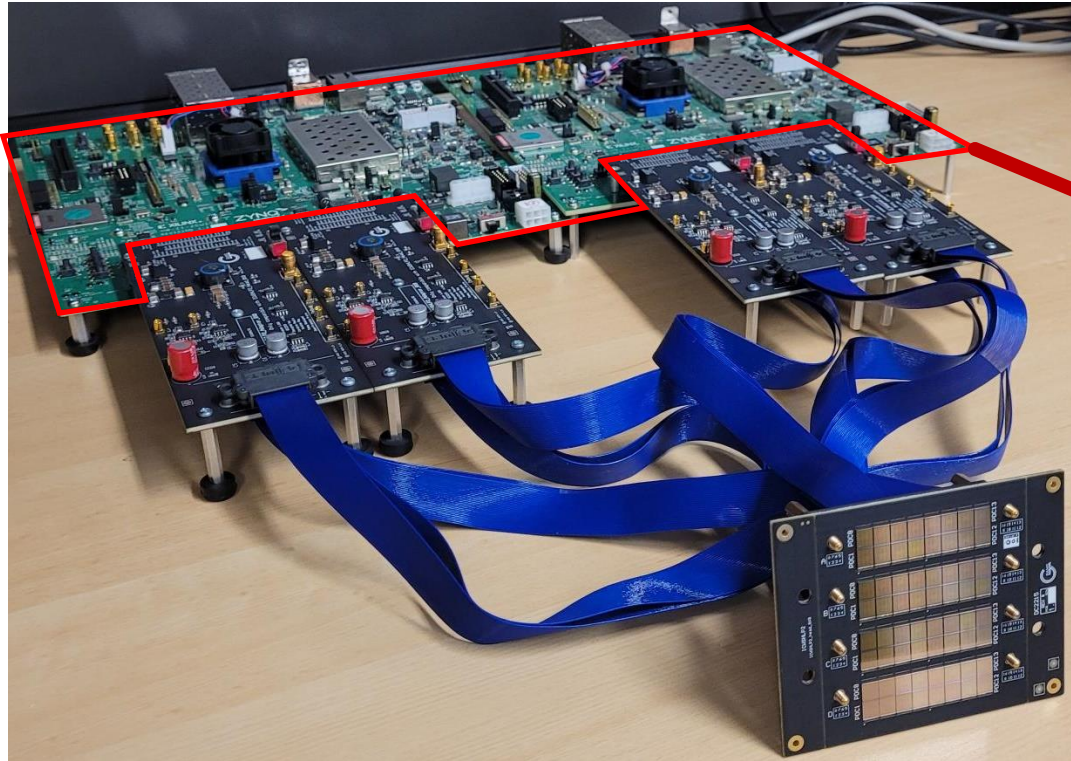
300 tonnes of LAr – 250 m² of photon detectors

Our global ambition

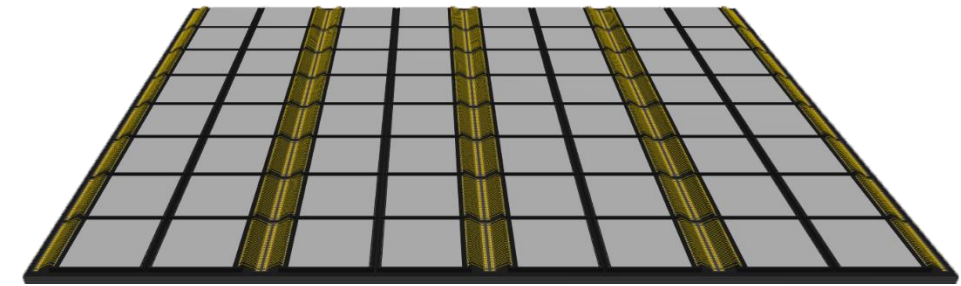


- Demonstrated small tile prototypes
- Silicon interposer for low background large scale integration
- Optical (digital) communication
- Embedded time-to-digital conversion

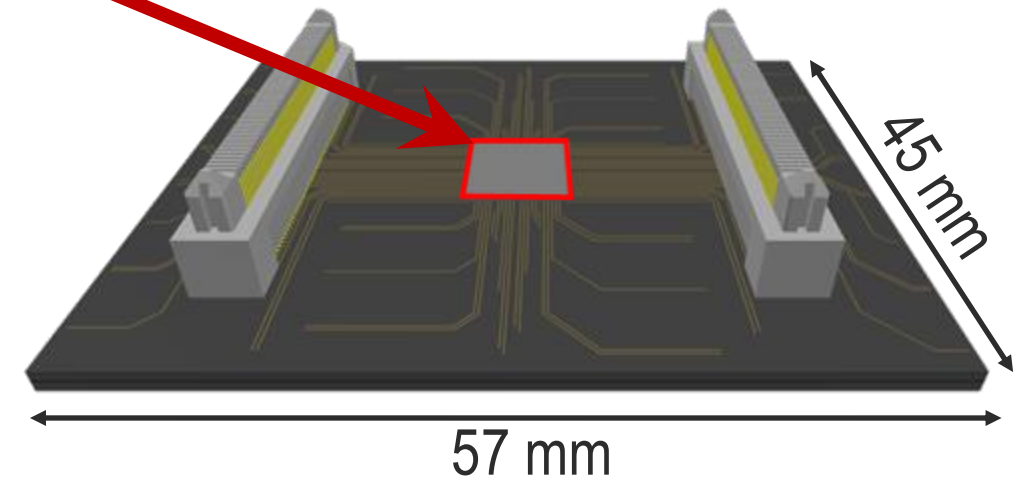
FPGA-based Controller



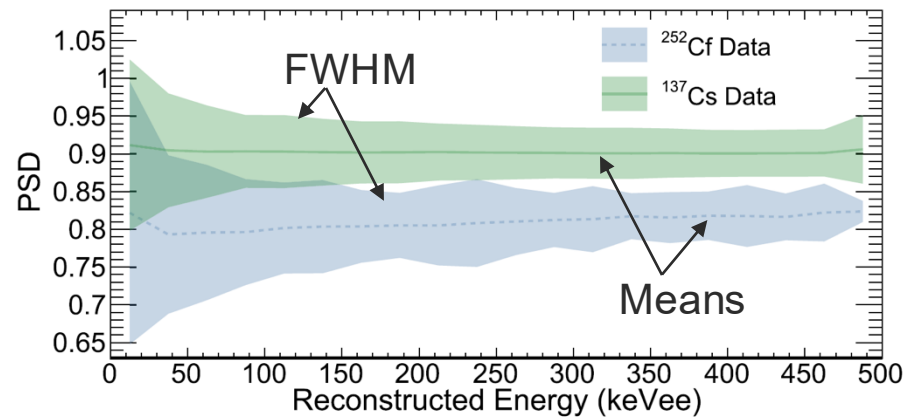
ASIC-based Controller



Top side

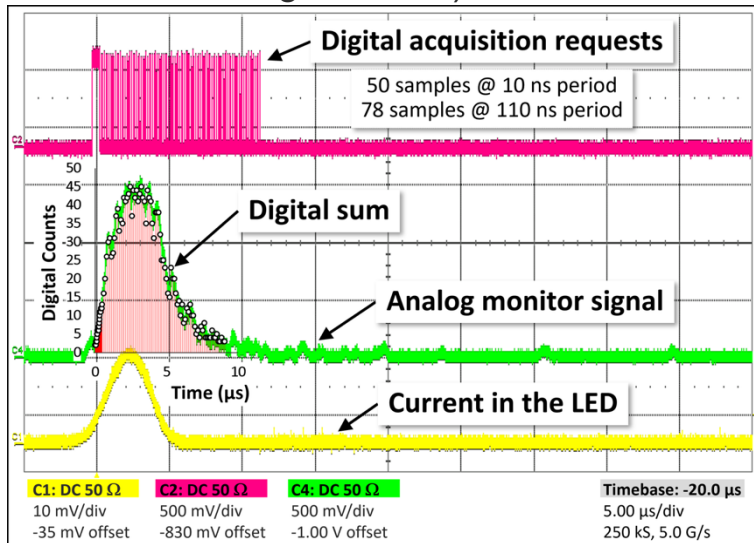


Bottom side

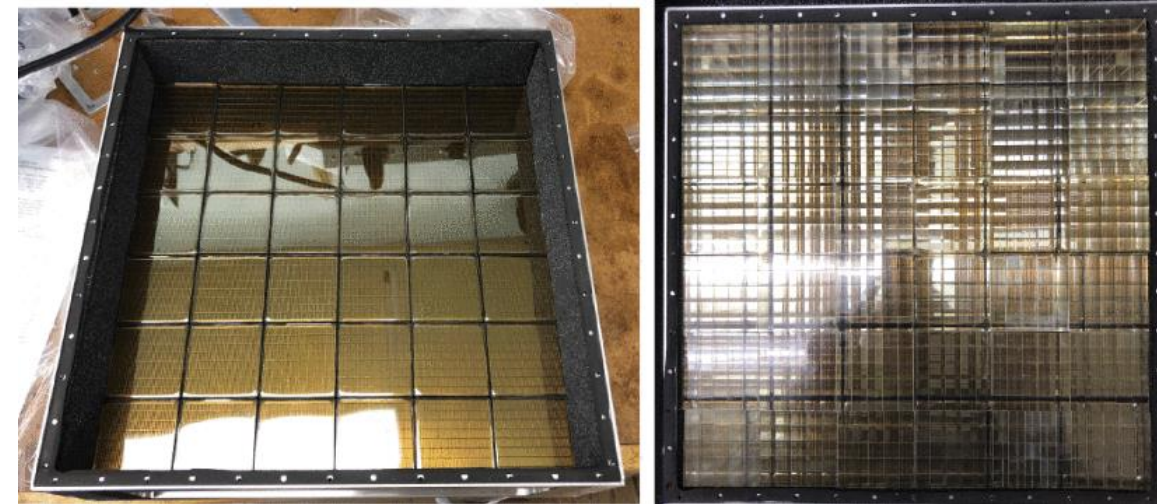
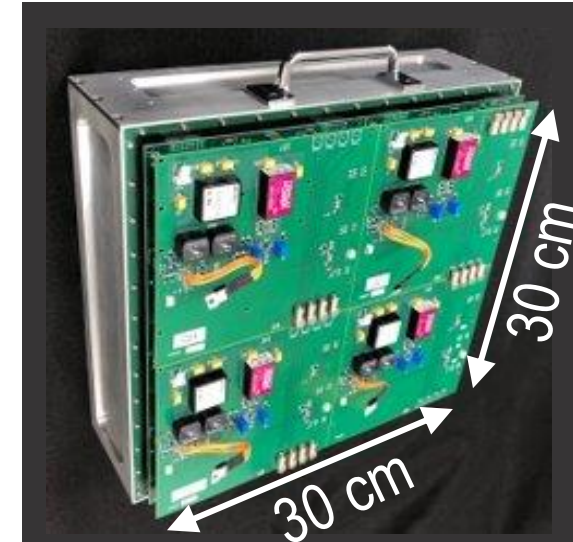


PSD parameter as a function of energy. [1]

Capability of the PDC to measure PSD
(here simulated LED light source)



Goal:
next generation of portable
neutron detector panel



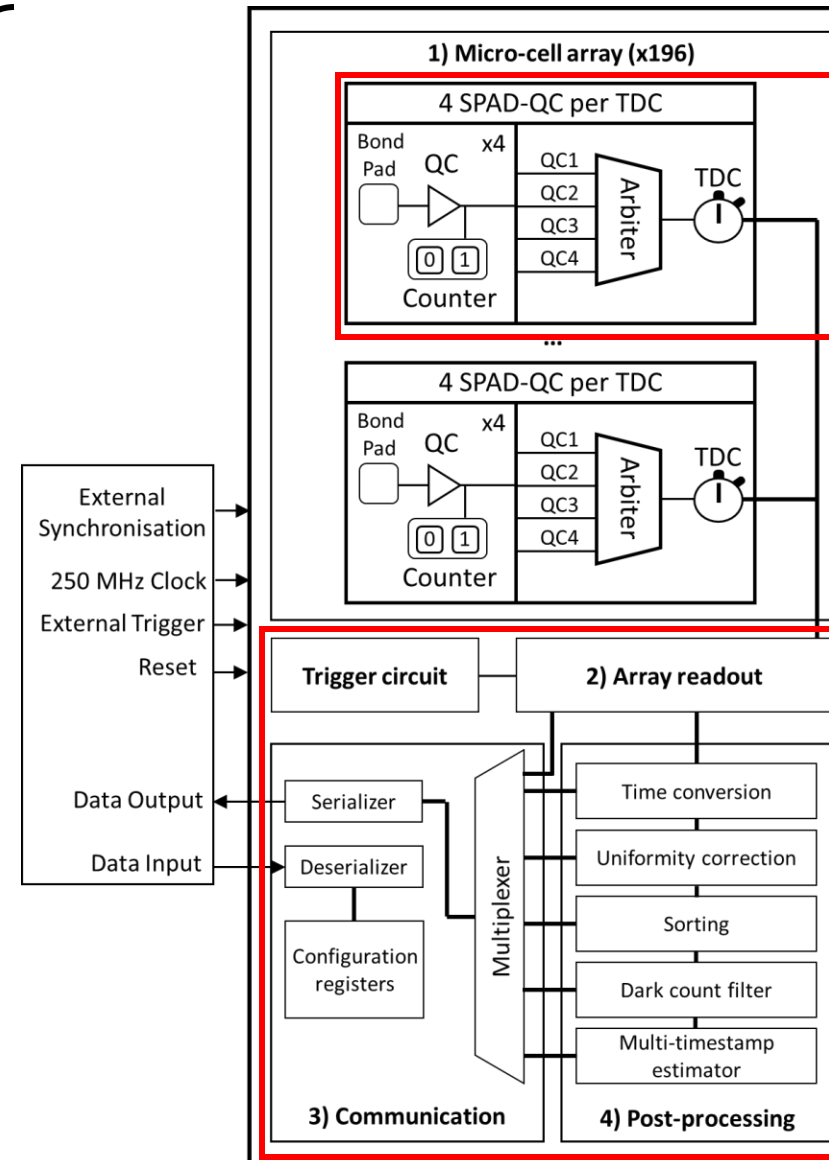
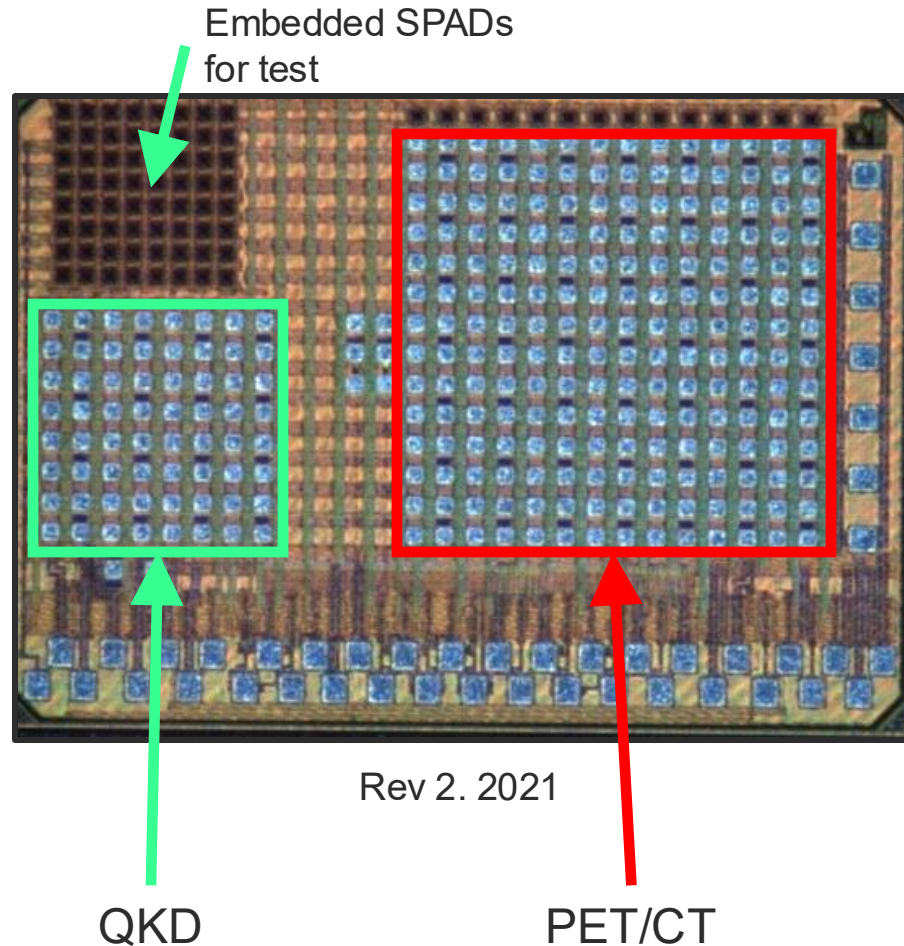
ORNL Portable Pixelated Fast-Neutron Imaging Panel [1]
Left: Multi-Anode PMT | Right: Pixelated scintillators



Photo-to-Digital Converters designed for precise timing applications

**Quantum key distribution,
Wavefront sensing,
Medical imaging ToF-PET, ToF-CT,
...**

- TSMC 65 nm CMOS
- 16×16 pixels in $1.1 \times 1.1 \text{ mm}^2$



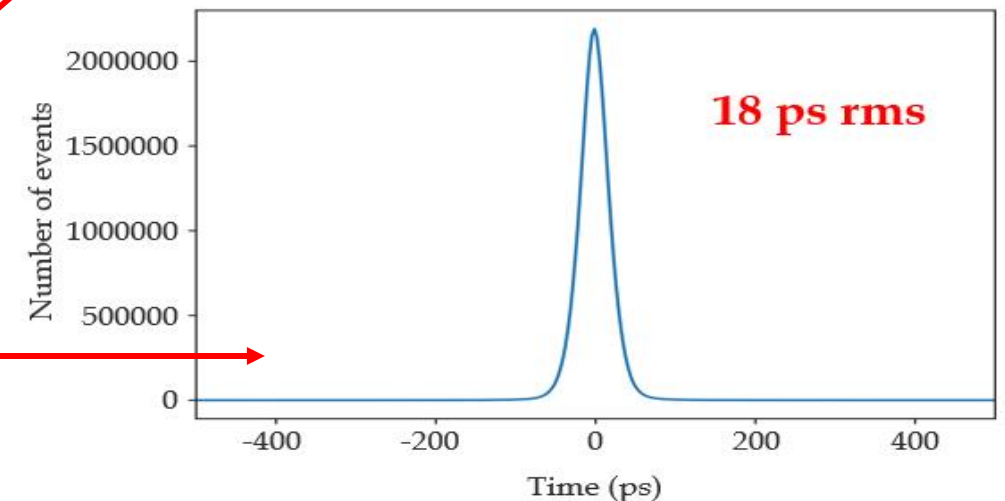
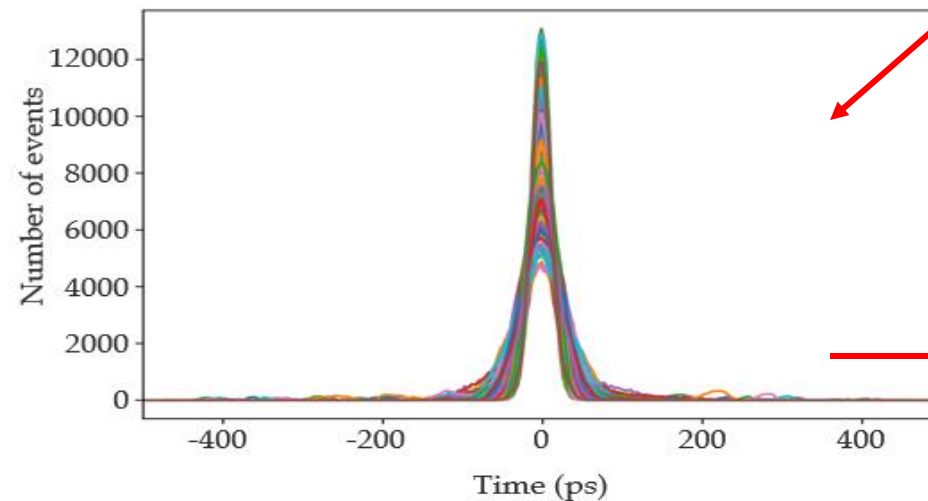
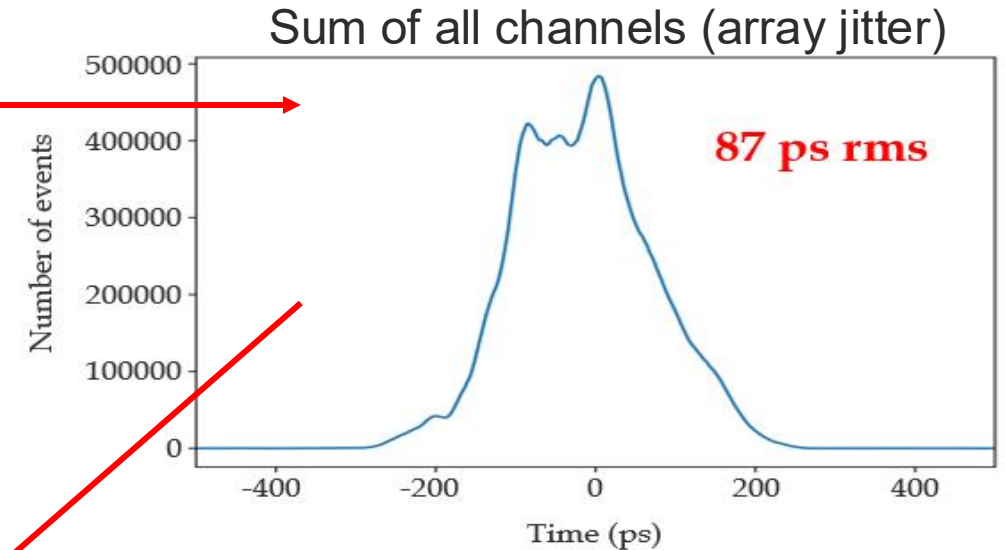
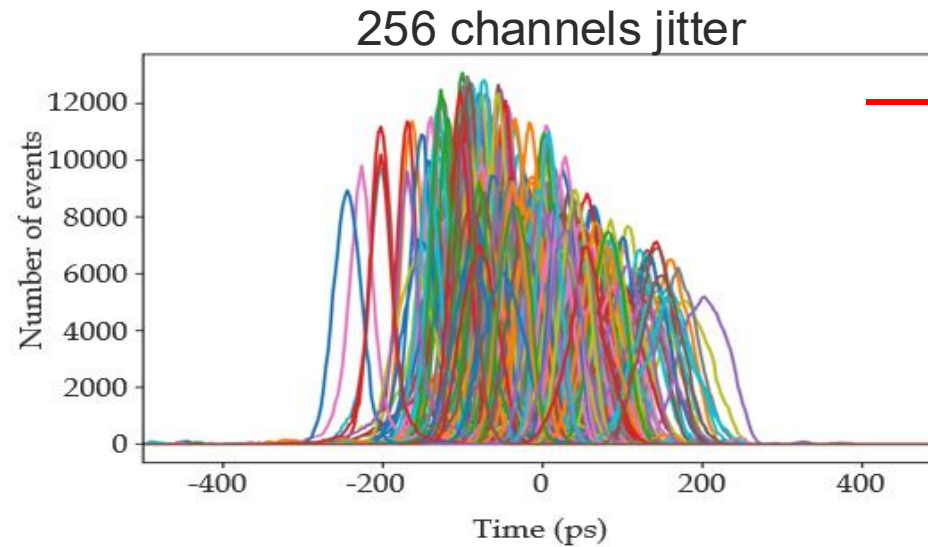
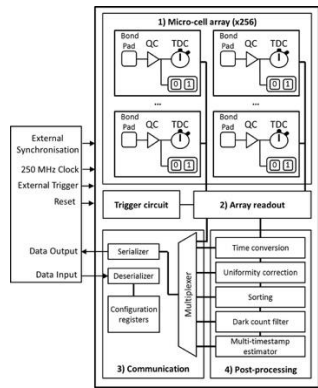
1 Sub-20 ps TDC for 4 SPADs

Advanced digital signal processing:

- Time windowing
- TDC code to time conversion
- Uniformity correction
- Timestamp sorting
- Dark count filtering
- BLUE

And for QKD

- Time categorization



A decorative green pattern on the left side of the slide, consisting of a repeating grid of stylized, interlocking wave or 'S' shapes in two shades of green.

ToF Computed Tomography

Using time-of-flight to exclude noise from scattering X-ray photons

ToF Scatter Rejection Principle

How do that?

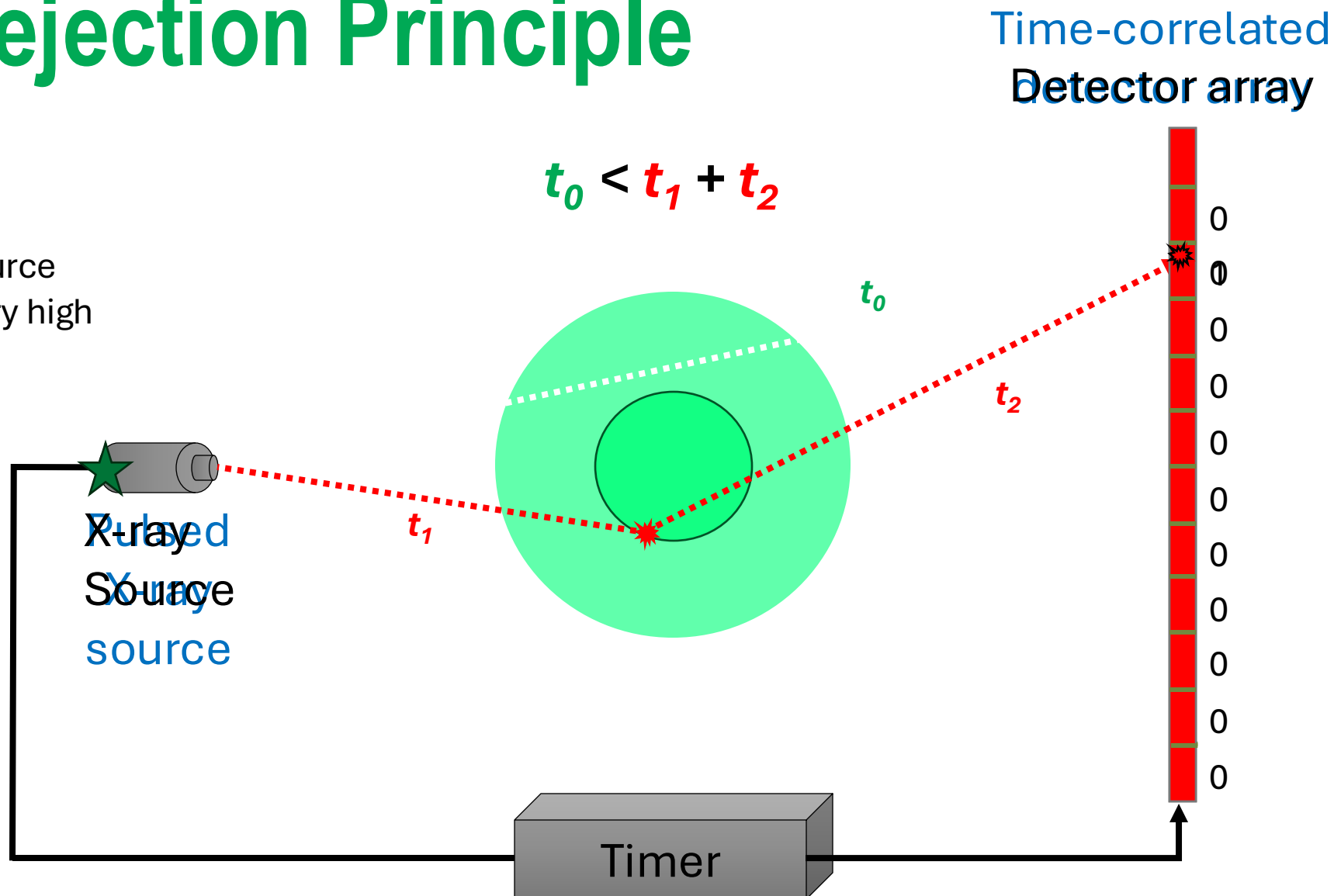
To do this we need:

- Synchronized pulsed X-ray source
- Time-resolved detectors of very high precision ($\sim 10\text{-}200$ ps FWHM)

Threshold for rejection:

$t_{th} \sim 10\text{-}500$ ps FWHM

$$t_1 + t_2 > t_0 + t_{th}$$



A decorative vertical bar on the left side of the slide, featuring a solid green background with a repeating pattern of stylized, light green, interlocking wave or 'S' shapes.

Quantum Key Distribution

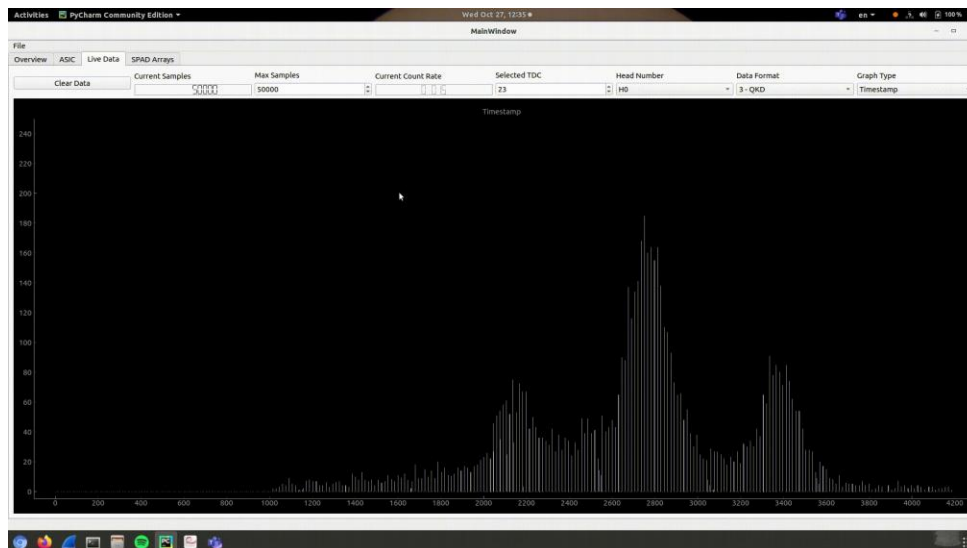
Exploiting in timestamp processing

Raw time stamp data

Each photon is timestamped in the chip

- ~20ps resolution and precision
- Timestamps are transmitted to the computer

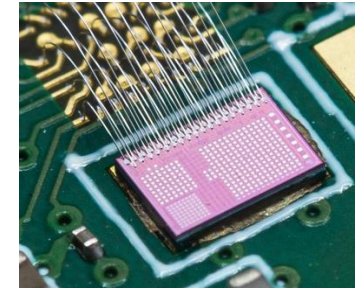
The histogram shows 3 modes to the distribution corresponding to the projection of the 4 states of the qubit onto the time base (center bin holds 2 states)



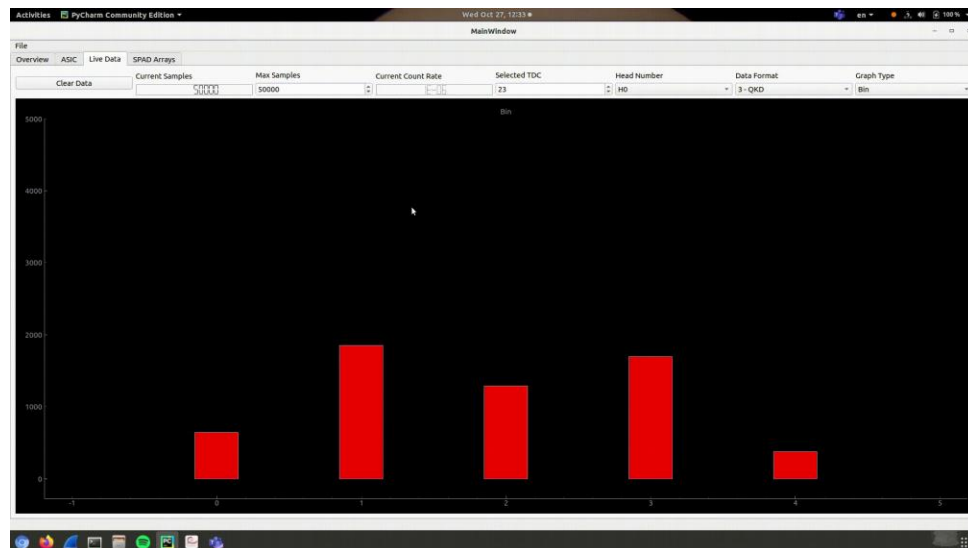
Classified time-bins

Timestamps are classified inside the chip into 5 bins

- Two bins for out-of-range values
- Programmable bins



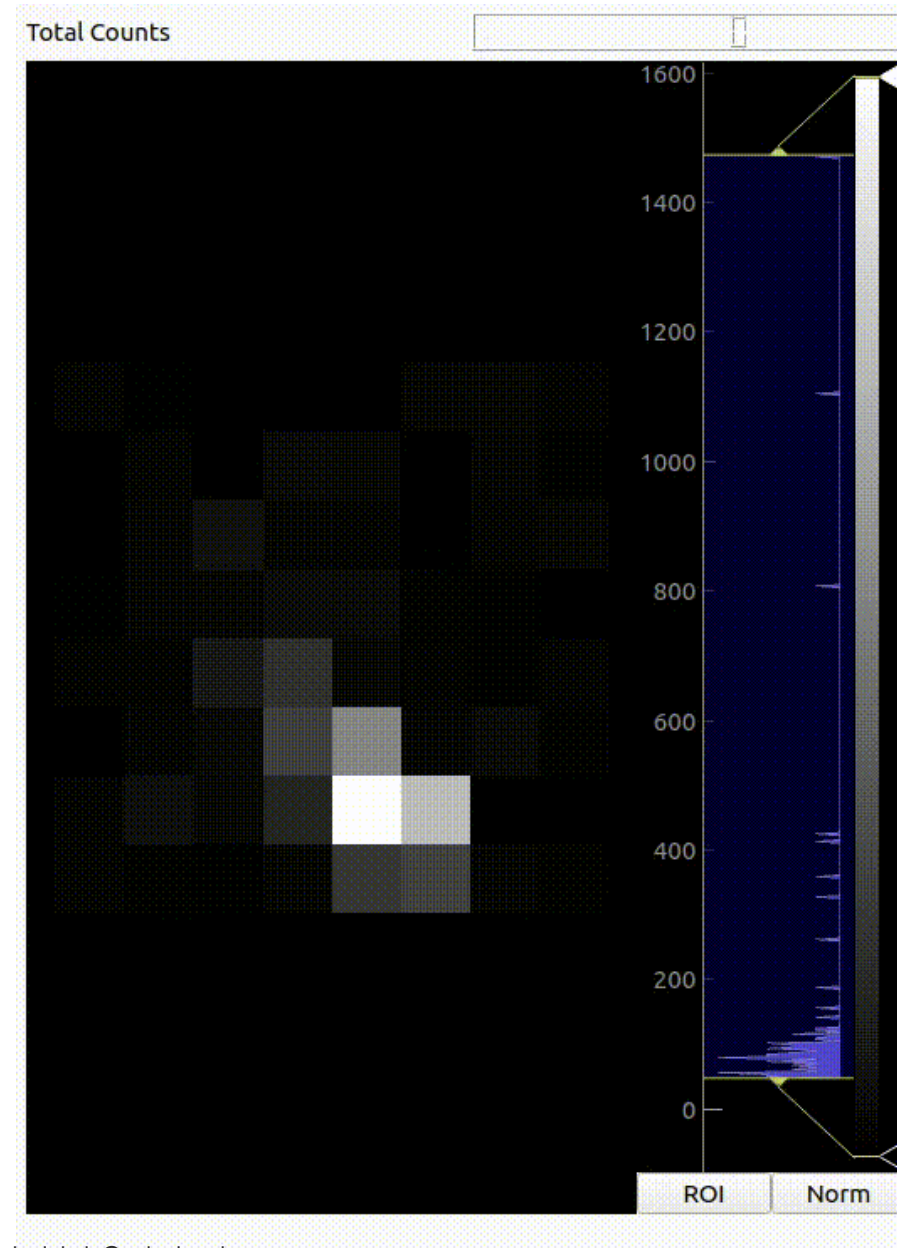
This provides effective data compression, limiting the relevant information to only 2-3 bits for each qubit



The two graphs show different measurements.

Time variations are due to slow tuning of polarizer/interferometer for the purpose of this demonstration.

- Applied in an array we get
 - The timestamps or time bins
- AND
- Photon location on the array

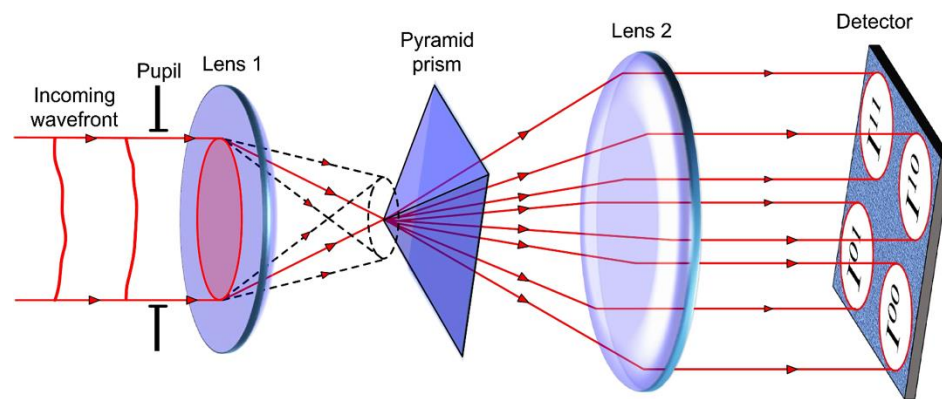




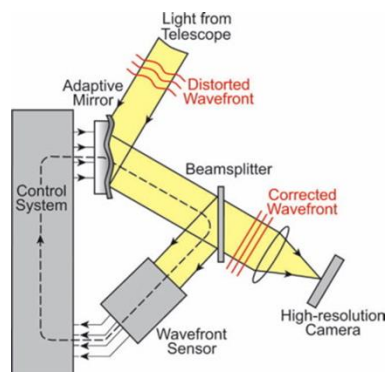
Rapid Wavefront Sensing

For exoplanet search

Pyramidal Wavefront Sensing for AO



Shatokhina et al. 2020 [10.1117/1.JATIS.6.1.010901](https://doi.org/10.1117/1.JATIS.6.1.010901)

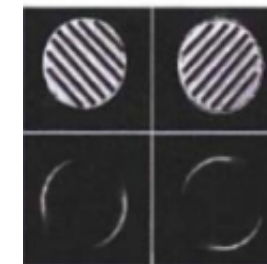
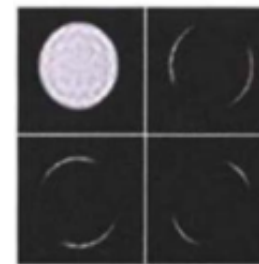
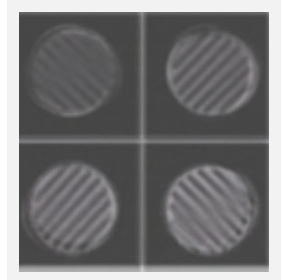


Conventional Pyramid WaveFront Sensing (PWFS)

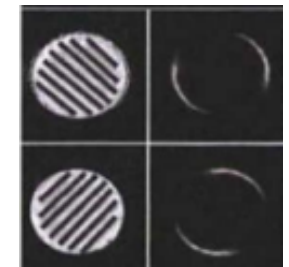
- Integrates photons over a modulation cycle

Time-resolved PWFS

- Separates a modulation cycle into 48 frames
- Because each frame captures one diffraction pattern
 - Increases signal to noise ratio



...





Conclusion

• 3D Photon-to-Digital Converters in fabrication

- PDC fabrication runs planned every 4-6 months
 - Increasing the manufacturability,
 - Tuning/exploring performance improvements
- PDC now being assembled on test boards (instead using probing station)

• Dissemination of test platforms to collaborators

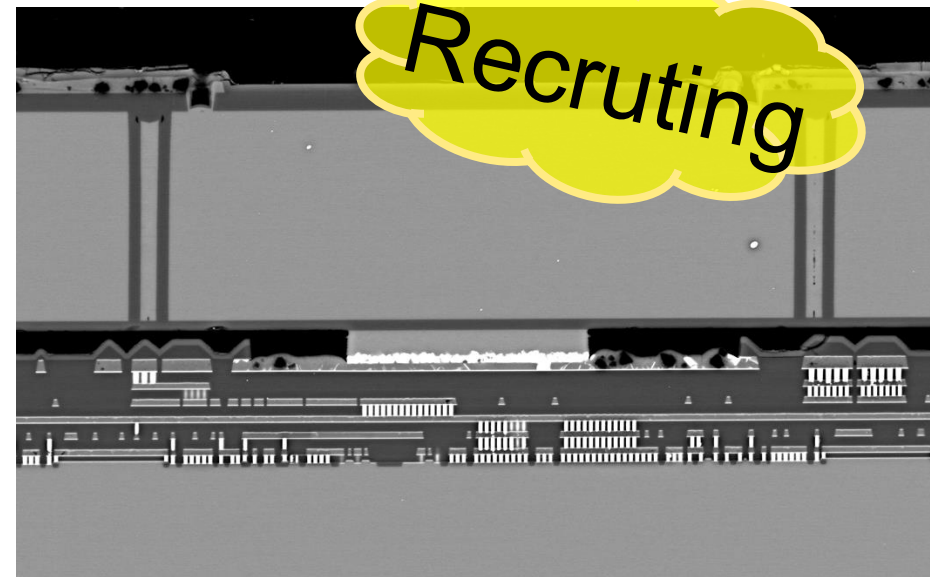
- Training on CMOS-only boards
- PDC boards should be available Fall 2025

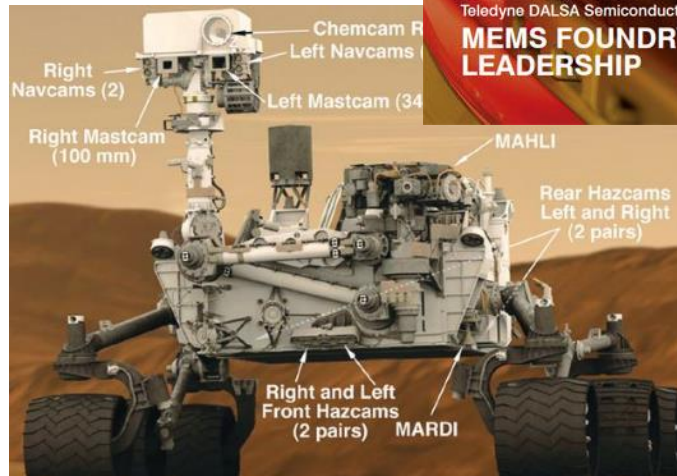
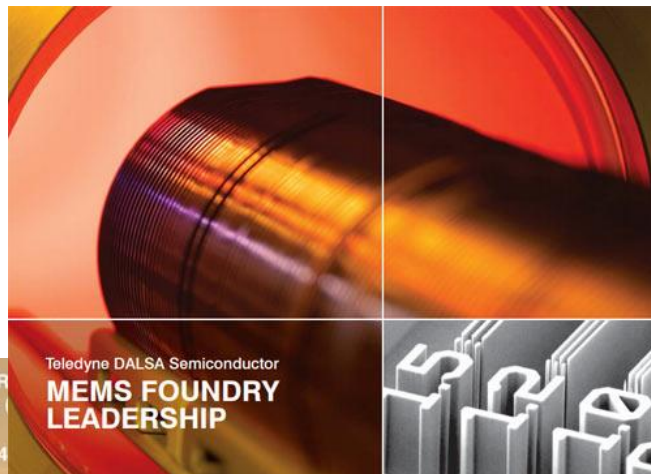


MI supported

• High performance Photon-to-Digital Converter

- Small array demonstrated: quenching $\sigma < 5$ ps, TDC $\sigma < 10$ ps
- Completing design/validation of 5×5 mm² array → 2026
 - Readout prototyping → 2026
- Wafer level 3D assembly with SPADs → 2027





L'U_{de}S fait partie des 10
plus grandes universités
de recherche au Canada

On PDC development

- T. Rossignol et al., “A 3D photon-to-digital converter readout for low-power and large-area applications,” J. Inst., vol. 19, no. 09, p. P09017, Sep. 2024, doi: 10.1088/1748-0221/19/09/P09017.
- S. Parent et al., “Wafer-Level Characterization and Monitoring Platform for Single-Photon Avalanche Diodes,” IEEE J. Electron Devices Soc., vol. 12, pp. 127–137, 2024, doi: 10.1109/JEDS.2024.3359088.
- J.-F. Pratte et al., “Fast neutron radiography-based on single-photon digital photosensor: concept and demonstration,” in Hard X-Ray, Gamma-Ray, and Neutron Detector Physics XXV, N. J. Cherepy, M. Fiederle, and R. B. James, Eds., San Diego, United States: SPIE, Oct. 2023, p. 12. doi: 10.1117/12.2682610.
- F. Nolet et al., “Quenching Circuit Discriminator Architecture Impact on a Sub-10 ps FWHM Single-Photon Timing Resolution SPAD,” Instruments, vol. 7, no. 2, p. 16, Apr. 2023, doi: 10.3390/instruments7020016.
- S. Carrier et al., “Towards a Multi-Pixel Photon-to-Digital Converter for Time-Bin Quantum Key Distribution,” Sensors, vol. 23, no. 7, p. 3376, Mar. 2023, doi: 10.3390/s23073376.
- Rossignol, T. “Conception d’un circuit de lecture d’une matrice de photodiodes à avalanche monophotonique pour les détecteurs de physique des particules dans les gaz nobles liquéfiés”. Dissertation, Université de Sherbrooke, 2020.

On ToF CT

- D. Gaudreault, J. Rossignol, Y. Bérubé-Lauzière, and R. Fontaine (2021), IEEE Transactions on Radiation and Plasma Medical Sciences, vol. 5, no. 3, pp. 343–349
- J. Rossignol, G. Bélanger, D. Gaudreault, A. C. Therrien, Y. Bérubé-Lauzière, et R. Fontaine, « Time-of-flight scatter rejection in x-ray radiography », Phys. Med. Biol., vol. 69, no 5, p. 055027, mars 2024, doi: [10.1088/1361-6560/ad1f85](https://doi.org/10.1088/1361-6560/ad1f85).
- J. Rossignol, G. Bélanger, M. Fromont, A. C. Therrien, R. Fontaine, et Y. Bérubé-Lauzière, « Scatter estimation and correction using time-of-flight and deconvolution in x-ray medical imaging », Phys. Med. Biol., vol. 69, no 17, p. 175017, sept. 2024, doi: 10.1088/1361-6560/ad700e.
- G. Belanger, J. Rossignol, , Y. Berube-Lauziere, and R. Fontaine (2024), To be published

On ToF PET

- Pratte, J.-F., et al. "3D Photon-to-Digital Converter for Radiation Instrumentation: Motivation and Future Works" (2021) Sensors;21(2):598. doi: 10.3390/s21020598
- Parent, S., et al. "Single photon avalanche diodes and vertical integration process for a 3D digital SiPM using industrial semiconductor technologies." 2018 IEEE Nuclear Science Symposium and Medical Imaging Conference Proceedings (NSS/MIC). IEEE, 2018.
- Parent, S., et al. "Characterization and Monitoring Platform for Single-Photon Avalanche Diodes in the Development of a Photon-to-Digital Converter Technology.", 2022 IEEE International Conference on Microelectronic Test Structures Proceedings (ICMTS). IEEE, 2022.
- Parent, S., "Design of a Vertically Integrated Single-Photon Avalanche Diodes, Manufactured at Wafer level, for a Photon-to-Digital Converter Technology", PhD Thesis (to be published), 2022.
- Nolet, F. et al., "Quenching Circuit and SPAD Integrated in CMOS 65 nm with 7.8 ps FWHM Single Photon Timing Resolution", Instruments 2018, 2, 19.
- Nolet, F. et al., "Digital SiPM channel integrated in CMOS 65 nm with 17.5 ps FWHM single photon timing resolution", Nuclear Instruments and Methods in Physics Research Section A, 912, 29-32, 2018.
- Nolet, F. et al., "A 256 Pixelated SPAD readout ASIC with in-Pixel TDC and embedded digital signal processing for uniformity and skew correction", Nuclear Instruments and Methods in Physics Research Section A, 949, 162891, 2020.
- Lemaire, W. et al., "Embedded time of arrival estimation for digital silicon photomultipliers with in-pixel TDCs", Nuclear Instruments and Methods in Physics Research Section A, 959, 163538, 2020.
- Roy, N., et al. "Low Power and Small Area, 6.9 ps RMS Time-to-Digital Converter for 3-D Digital SiPM", IEEE Transactions on Radiation and Plasma Medical Sciences, 1(6) 2017.
- Therrien, A. C., et al. "Energy discrimination for positron emission tomography using the time information of the first detected photons", Journal of Instrumentation, 13, 2018.
- Loignon-Houle, F., et al., "DOI estimation through signal arrival time distribution: a theoretical description including proof of concept measurements", Physics in Medicine and Biology, 66(9), pp. 095015, 2021.



Extras



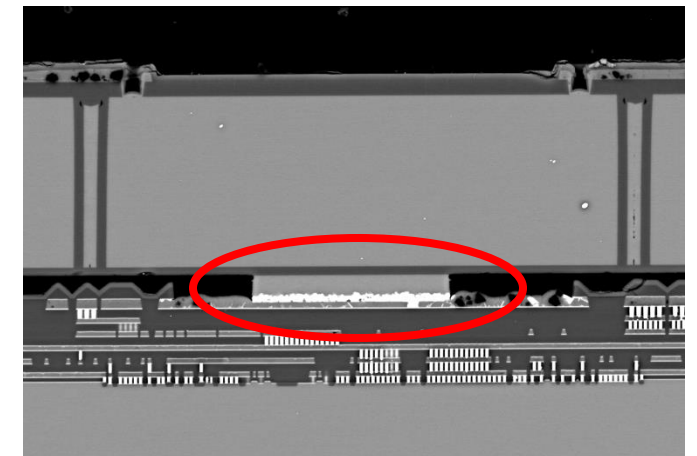
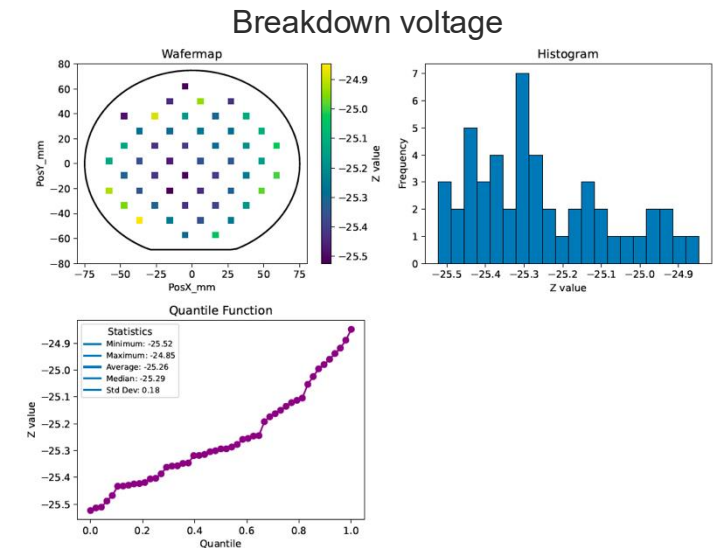
First PDC Characterization Results

Completion of the first 3 wafers of PDC

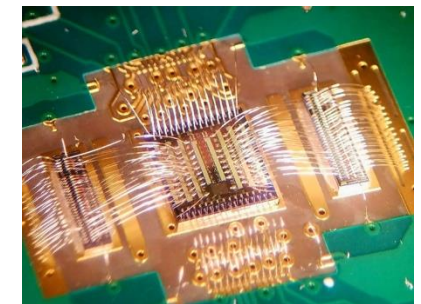
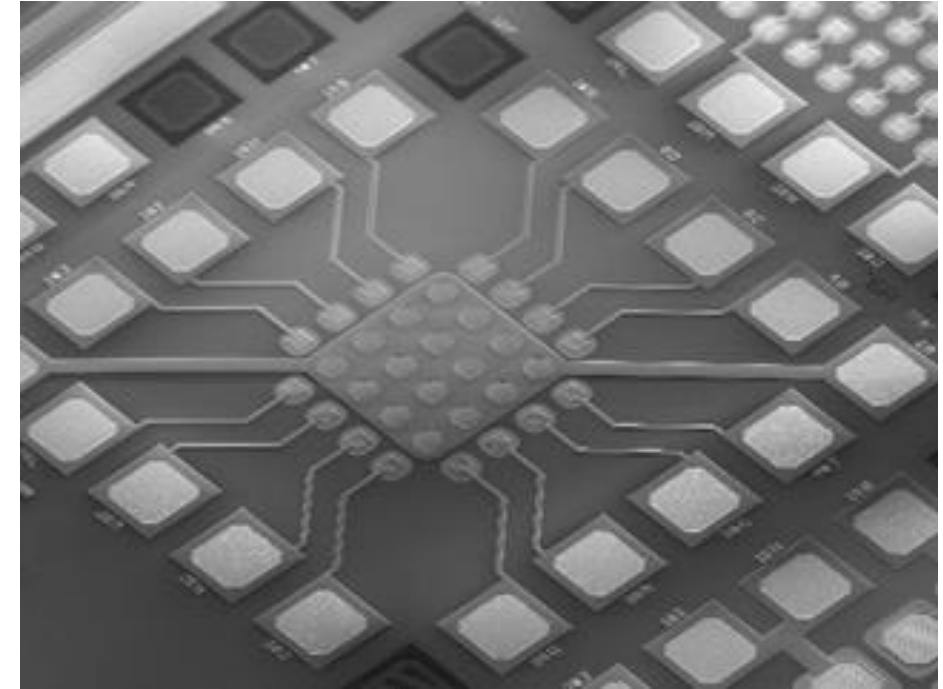
- 1st run: Delivered on Oct. 13th 2024 (3 wafers)
- 2nd run: Delivered on April 29th 2025 (2 wafers)

Process control monitor results:

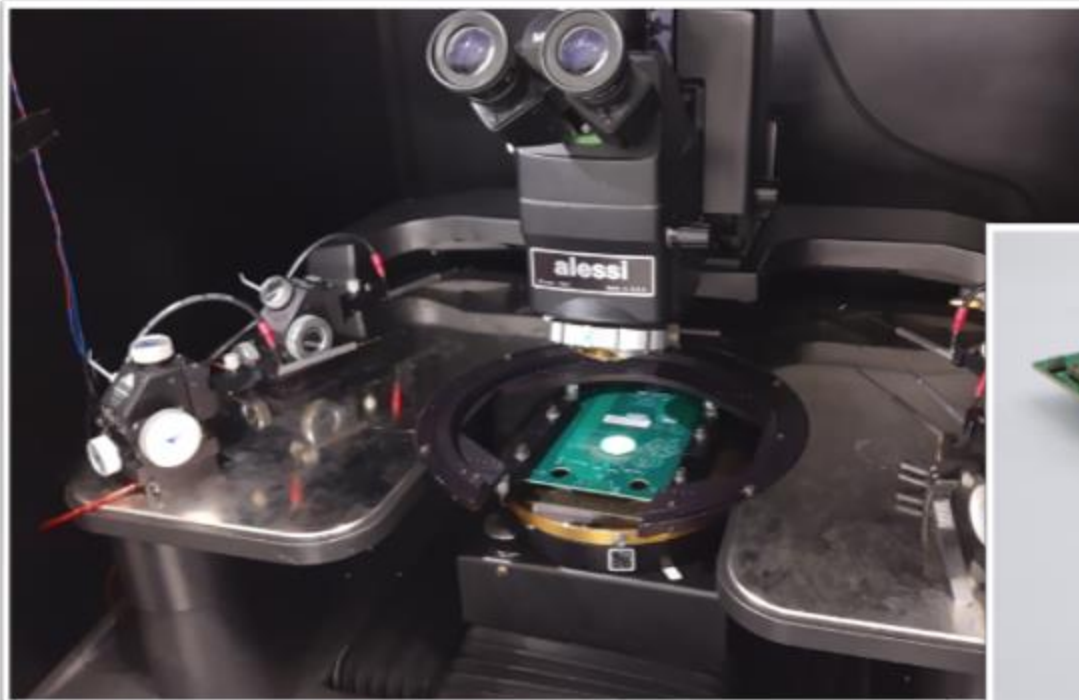
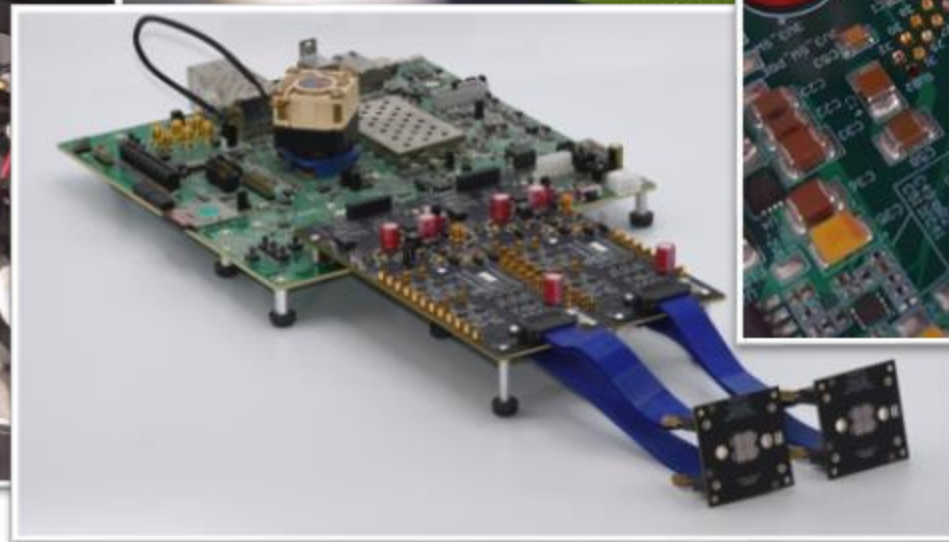
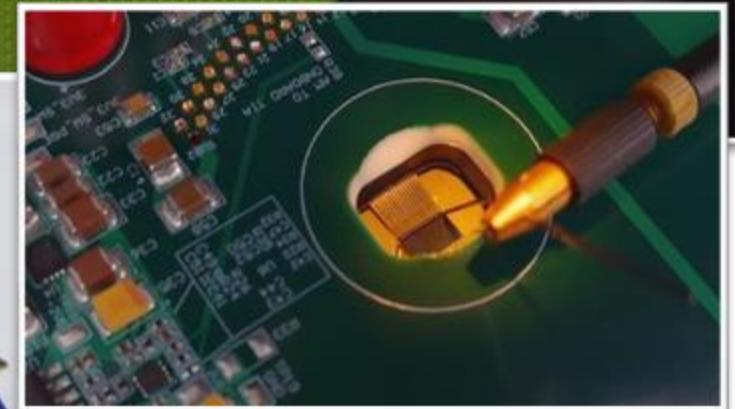
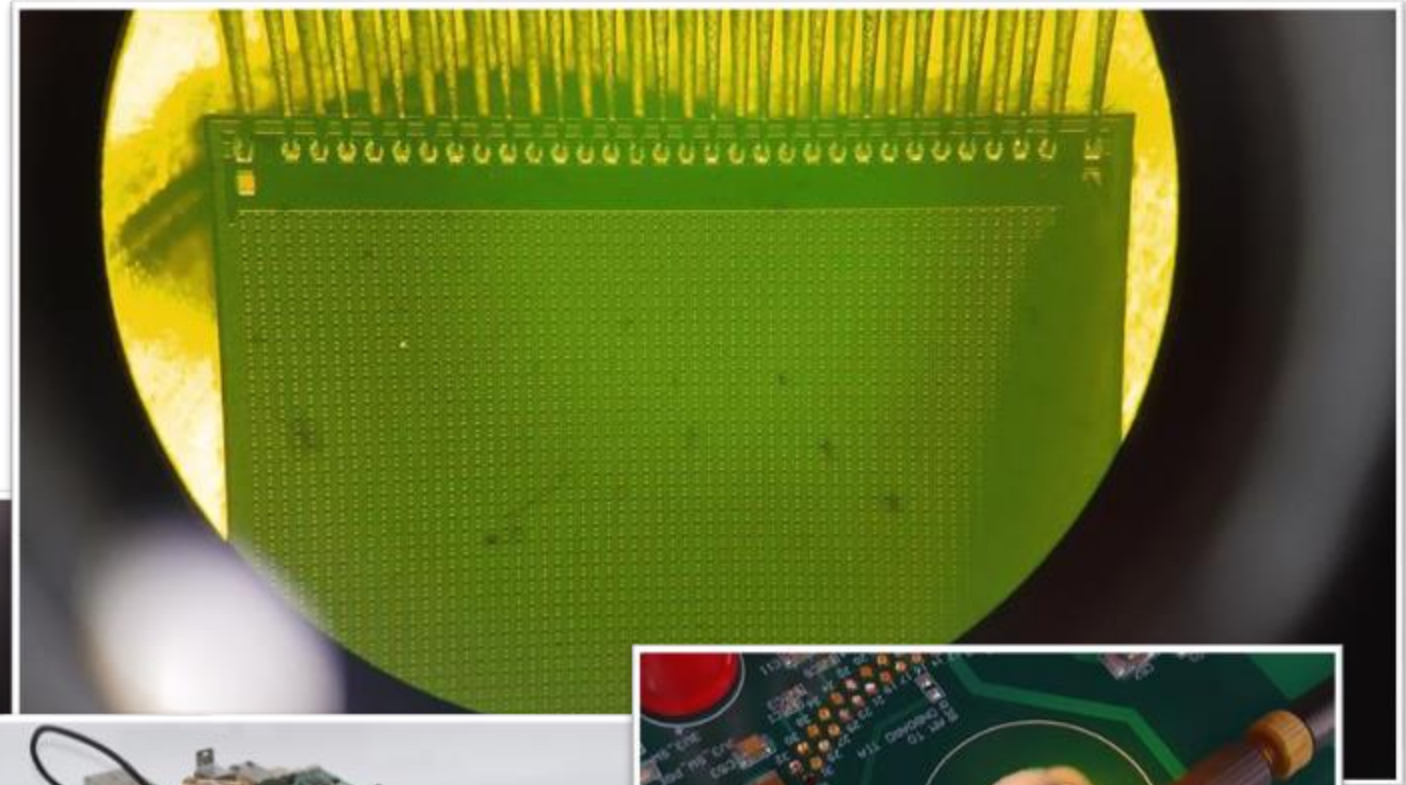
- Standard foundry process monitoring structures
 - All in specs on all wafers (~30 types of tests)
- SPAD performances: comparable to our previous SPAD runs
 - Breakdown voltage on specifications: $25.26\text{V} \pm 0.18\text{V}\sigma$ (@ $1\mu\text{A}$ bias)
 - DCR ~ 50-60 cps/SPAD @ 20-25% V_{ex} @ RT \rightarrow ~ 0.03 cps/ μm^2
 - Afterpulsing $\sim 1.3\%$
- SPAD-to-Quench connection yield > 99.8%
 - Only 30 defective structures out of 980 (47040 contacts)



- Testing individual SPADs of a small array
 - SPADs with trenches, nominally identical to those in PDCs
 - Anode routed to top surface (resistive vias)
- Crosstalk – ongoing
 - Enabling one or two SPADs and comparing count rate
 - **Preliminary:** ~10%
 - **To come:** study through time delay distributions
- SPTR measurement – ongoing
 - External quenching slows response and increases SPTR
 - **Preliminary:** 70 to 150 ps (wavelength dependant), comparable to 2023 results
 - **To come:** measurements on the PDC itself with local quenching

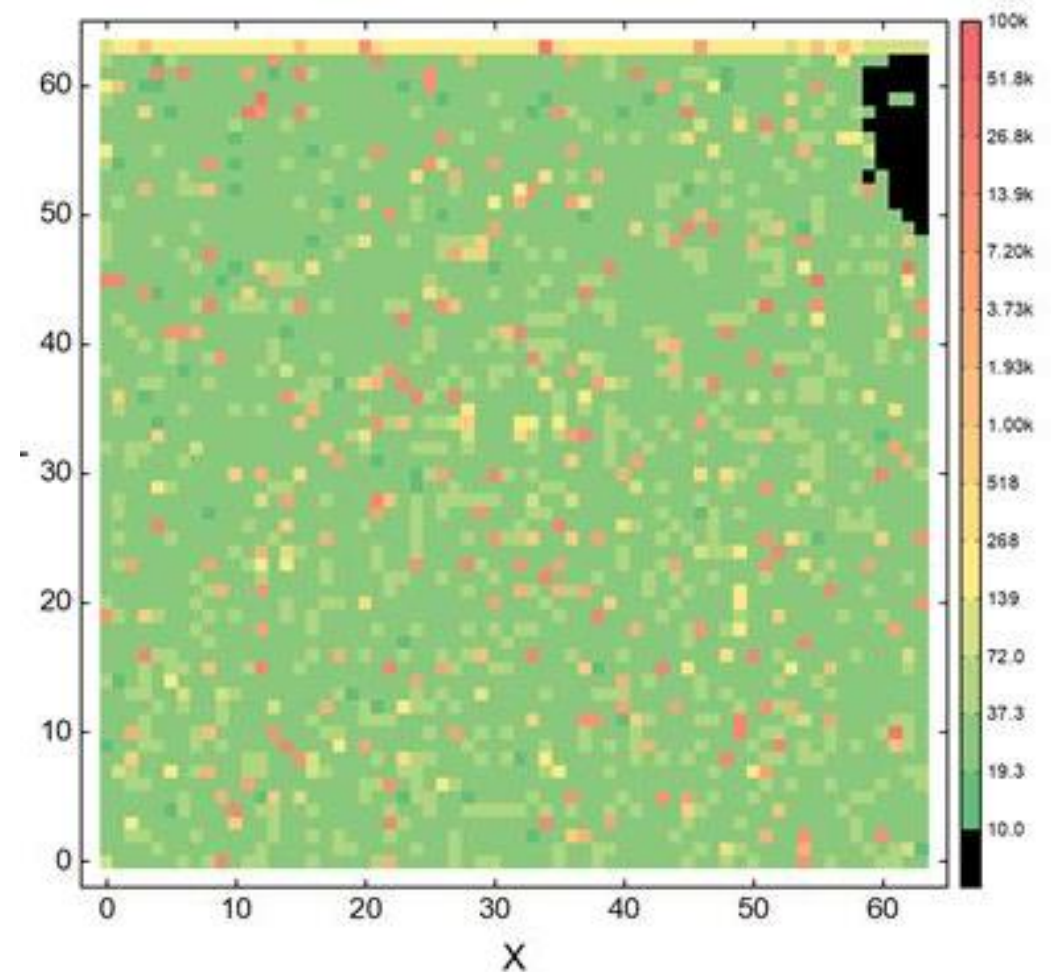


- Active testing of PDC performed with FPGA controller board*
- Flat cable connecting a probe card
- Ethernet connection to DAQ computer

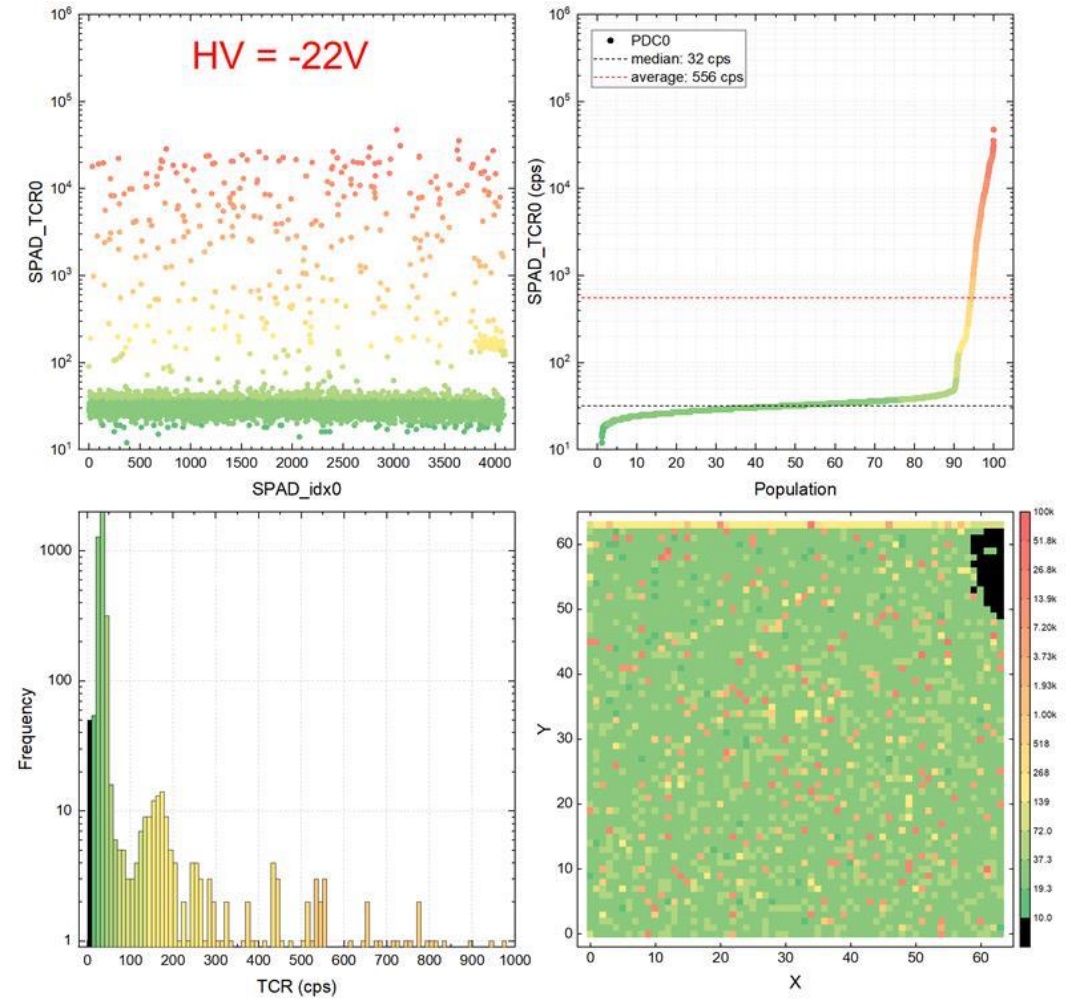


- Scan of all 4096 SPADs of the PDC
 - Activate a single SPAD
 - Therefore no crosstalk contribution in this measurement
 - Count “events” over one second → TCR
 - In this map: using flag output and counter in FPGA
 - Also possible: use the numeric sum (to come)

Map of total count rate (DCR+AP)
per SPAD (4096)

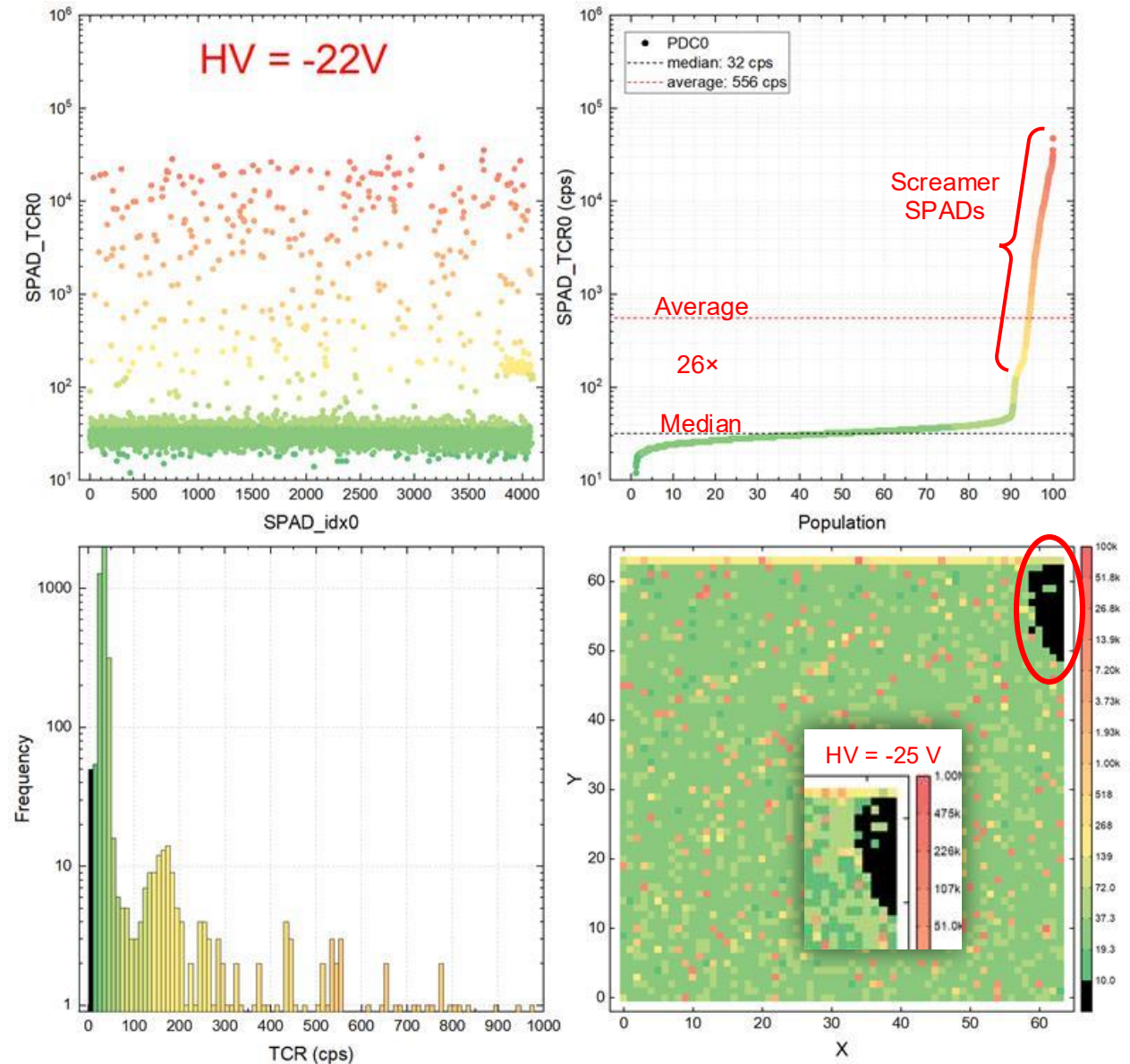


- Scan of all 4096 SPADs of the PDC
 - Activate a single SPAD
 - Therefore no crosstalk contribution in this measurement
 - Count “events” over one second → TCR
 - In this map: using flag output and counter in FPGA
 - Also possible: use the numeric sum (to come)
- Upper left: SPAD index mapping
- Upper right: Population ordered by TCR
 - Allow identifying the “screamer” sub-population and its impact on overall TCR
- Bottom left: TCR histogram

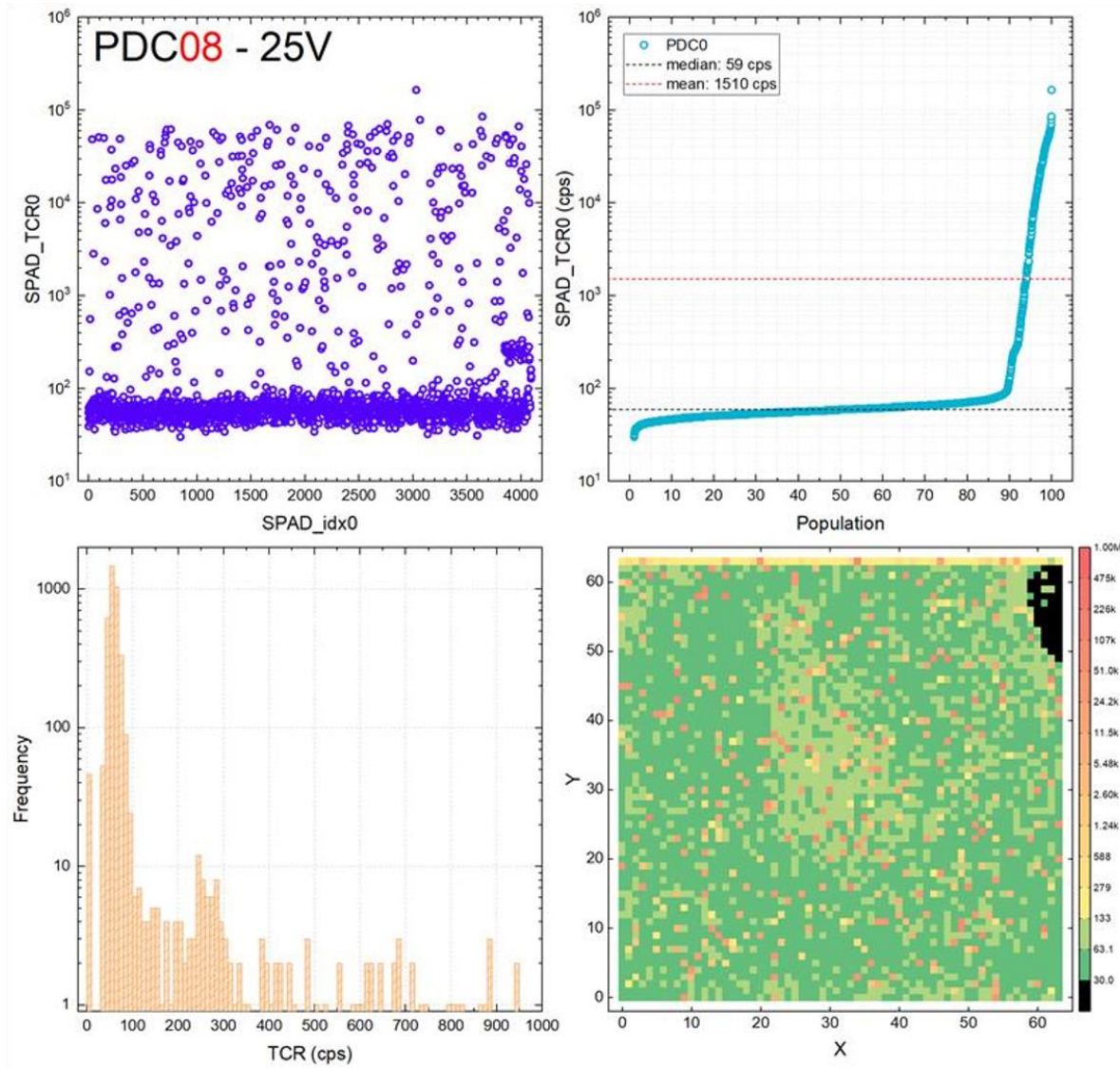


Four ways to look at the data to get a PDC's “unique” fingerprint

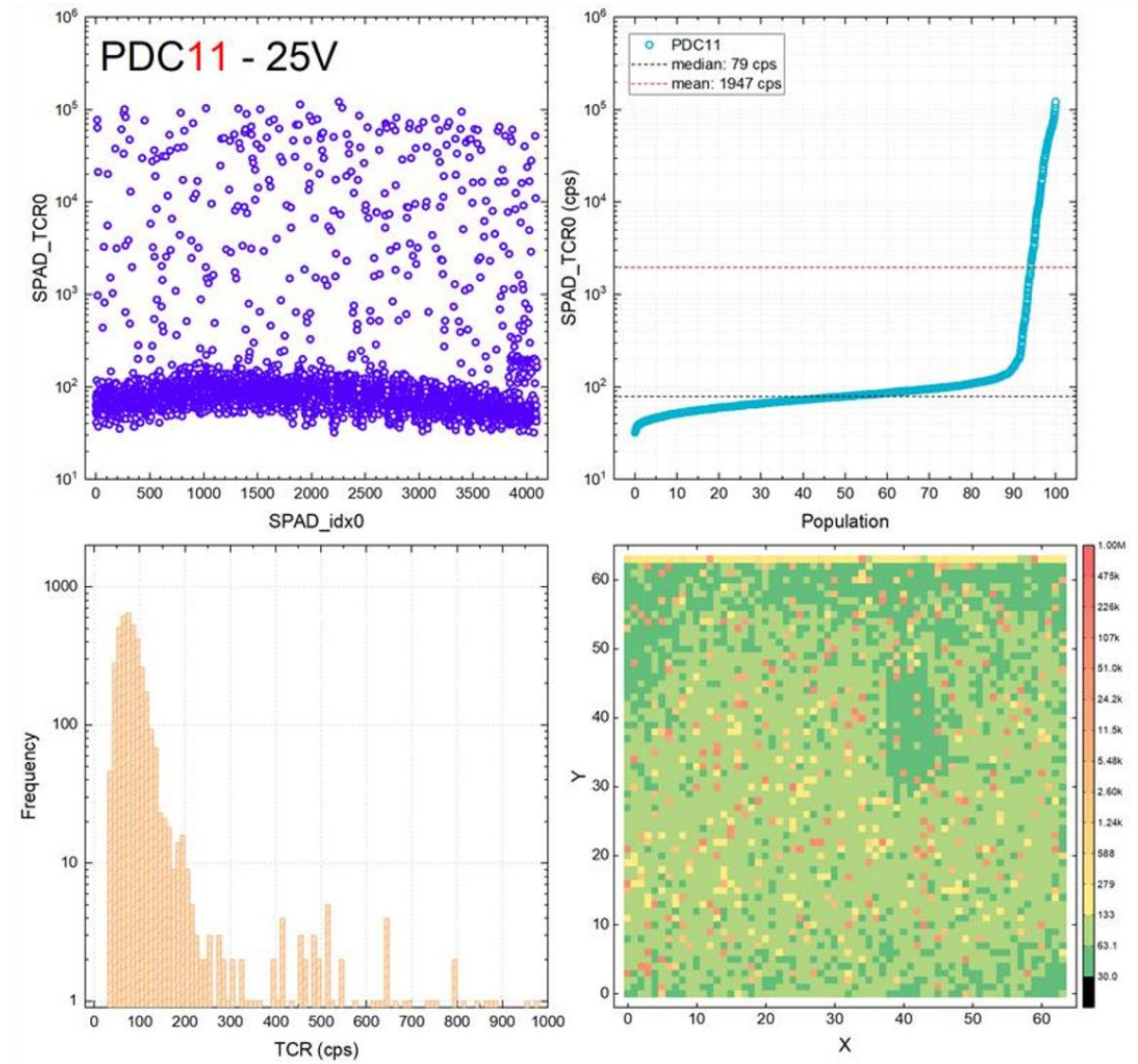
- 4096 SPADs in a 64×64 array
- 46 SPADs not responding (at -22 V bias)
 - 4 of these SPADs respond at -25 V bias
 - Under investigation
- Average TCR is dominated by screamers
 - 5% to 7% of population (depends on definition)
 - Median TCR is 26× lower than average TCR
 - Typical from literature, also expected in SiPMs



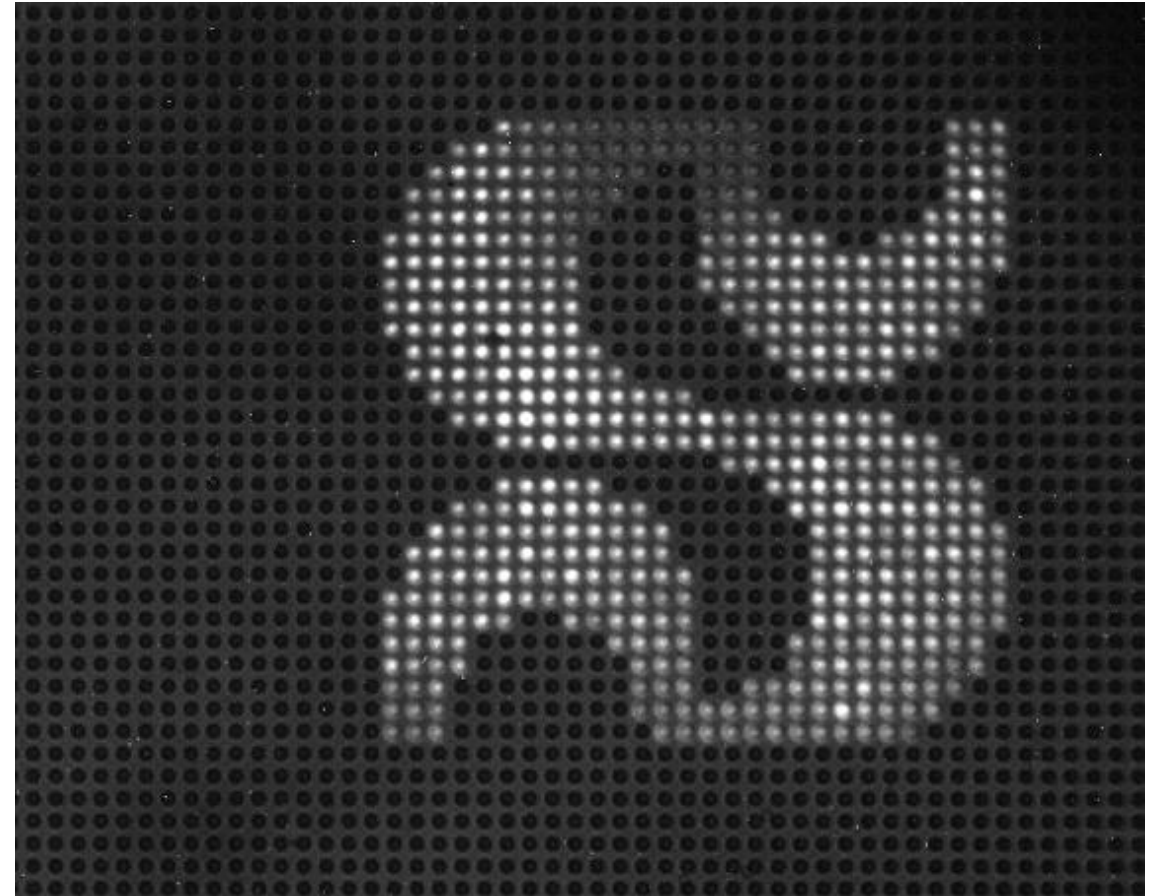
PDC08



PDC11

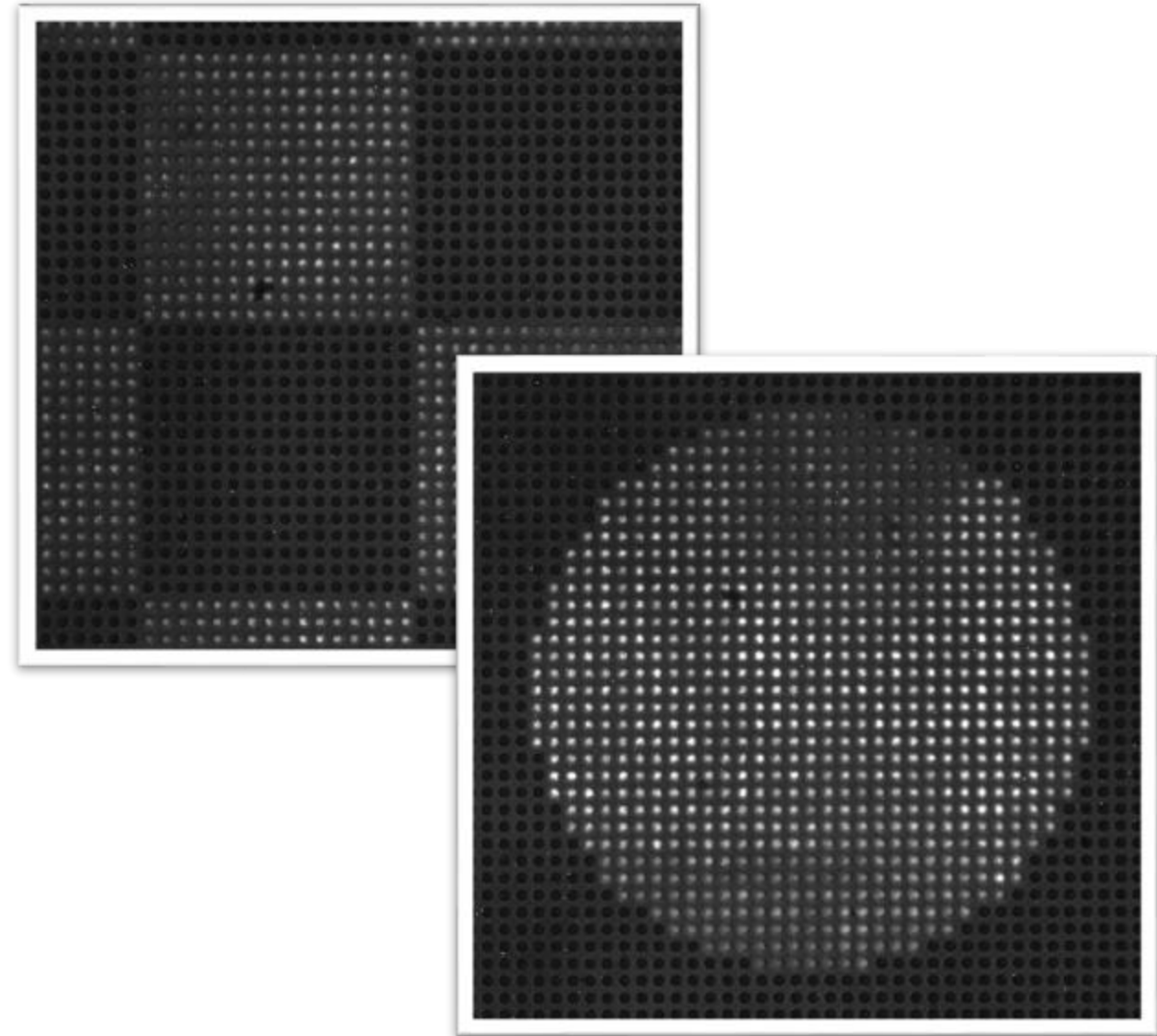


- During avalanche, SPADs emit light
 - Source of cross-talk both internal and external
- Demonstration of the capability of single SPAD activation/deactivation
 - SPADs forming a motif were activated
 - Long exposure of a sensitive camera reveals electroluminescence of the activated SPADs (here deliberately saturated to the show!)
 - Deactivated SPADs show no emission
- We will investigate the use of light emission to rapidly characterize PDC DCR



Light emission – PDC11 – 2 min exposure 24.5 V

- During avalanche, SPADs emit light
 - Source of cross-talk both internal and external
- Demonstration of the capability of single SPAD activation/deactivation
 - SPADs forming a motif were activated
 - Long exposure of a sensitive camera reveals electroluminescence of the activated SPADs (here deliberately saturated to the show!)
 - Deactivated SPADs show no emission
- We will investigate the use of light emission to rapidly characterize PDC DCR



Light emission – PDC11 – 2 min exposure 24.5 V